

Realization of efficient quantum gates with a superconducting qubit-qutrit circuit

T. Bækkegaard,¹ L.B. Kristensen,¹ N.J.S. Loft,¹ C.K. Andersen,² D. Petrosyan,³ and N.T. Zinner^{1, 4, †}

¹*Department of Physics and Astronomy, Aarhus University, DK-8000 Aarhus C, Denmark.*

²*Department of Physics, ETH Zürich, CH-8093 Zürich, Switzerland*

³*Institute of Electronic Structure and Laser, FORTH, GR-71110 Heraklion, Greece.*

⁴*Aarhus Institute of Advanced Studies, Aarhus University, DK-8000 Aarhus C, Denmark.*

(Dated: March 15, 2022)

Building a quantum computer is a daunting challenge since it requires good control but also good isolation from the environment to minimize decoherence. It is therefore important to realize quantum gates efficiently, using as few operations as possible, to reduce the amount of required control and operation time and thus improve the quantum state coherence. Here we propose a superconducting circuit for implementing a tunable system consisting of a qutrit coupled to two qubits. This system can efficiently accomplish various quantum information tasks, including generation of entanglement of the two qubits and conditional three-qubit quantum gates, such as the Toffoli and Fredkin gates. Furthermore, the system realizes a conditional geometric gate which may be used for holonomic (non-adiabatic) quantum computing. The efficiency, robustness and universality of the presented circuit makes it a promising candidate to serve as a building block for larger networks capable of performing involved quantum computational tasks.

[†] correspondence should be addressed to N.T.Z. at zinner@phys.au.dk

Richard Feynman famously suggested to simulate quantum physics with quantum computers [1]. Fourteen years later, Seth Lloyd proved that an array of spins with tunable interactions indeed represents a universal quantum simulator [2]. Dynamically controlled spin chains can realize analog quantum simulations and digital quantum computations. Several physical systems are being explored for implementing tunable spin chains in the quantum regime, including trapped ions and atoms [3–5], quantum dots [6] and superconducting circuits [7, 8]. Over the last decade, superconducting circuits have steadily improved to become one of the most prominent candidates for the realization of scalable quantum computing [9–12]. With the development of the transmon qubit [13] and further advances, such as the 3D transmon [10], coherence times above 44 μ s [14–17] and per-step multi-qubit gate fidelity at the fault tolerance threshold for surface code error correction [18] have been achieved on multi-qubit devices [19].

Many approaches for entangling quantum gates with superconducting qubits have been implemented experimentally [19–27] and many more have been proposed theoretically [28–33]. Still, as the search for better coherence, lower error rates and faster quantum gate operation times continues, more efficient universal realizations of key operations for a quantum processor are needed. Most implementations so far have used only one- and two-qubit quantum operations for realizing important multi-qubit gates [34] such as the three-qubit quantum Toffoli [35] (CCNOT) and Fredkin [36] (CSWAP) gates, requiring a theoretical minimum of five two-qubit gates [34, 37, 38]. This large number of required gates can be remedied by the use of a higher-lying state of a qutrit which can simplify the implementation of e.g. the Toffoli gate to three two-qubit gates as implemented optically in [39] and in superconducting circuits in [40]. Moreover, the current implementations are highly specialized, meaning that the fabricated superconducting circuit is used just to implement a single three-qubit gate. A single circuit implementing several important universal quantum gates with high fidelity and minimal external control is therefore desirable.

Here, we propose a superconducting circuit realizing two qubits and a qutrit in between. First we show how the circuit can be used to generate two- and three-qubit entangled states [34, 41, 42]. Then we discuss how to implement the Fredkin gate using only two three-qubit operations, and the Toffoli gate using two (one-qubit) Hadamard gates and a three-qubit gate employing the intrinsic Ising-like ZZ (longitudinal) couplings and an external one-qubit driving. Finally we discuss how to implement a double-controlled universal unitary single-qubit gate. To illustrate this capability, we use the ZZ -couplings to realize the double-controlled holonomic gate [43, 44]. The geometric nature of the holonomic gate provides robustness but, the first proposals required adiabatic control leading to more time for errors to occur. The increase in errors was partly avoided by the introduc-

tion of decoherence-free subspaces [45], which can significantly reduce the detrimental effects of noise. We will instead implement a non-adiabatic generalization [46], circumventing many of these difficulties. Furthermore, we will show that this double-controlled gate can be used to implement the three-qubit Deutsch gate and is therefore universal for quantum computing in itself, adding yet another tool in our toolbox for efficient quantum gates.

RESULTS

Effective Hamiltonian of the system

Consider the circuit with four connected superconducting islands and the corresponding effective lumped circuit element model in Figure 1. The top-bottom symmetry between the capacitors and the Josephson junctions cancels the direct exchange interaction mediated by the capacitances and the leading order term from the Josephson junctions. On the other hand, we choose an asymmetry in the inductive couplings such that the difference between them controls the Heisenberg-like exchange coupling, which can be made arbitrarily small if so desired. Furthermore, while the exchange interaction mediated by the leading-order Josephson term ($E_{J1}/2$ in Supplemental Note 1) is canceled by symmetry, the dispersive (ZZ) coupling survives. The couplings are defined in Eq. (A61) and as seen in Supplementary Note 2, a ZZ coupling strength of ~ 30 MHz is realistic. Moreover, the ZZ coupling can be tuned in-situ by an external flux.

Using the effective lumped-element circuit of Figure 1b and following the standard procedure for circuit quantization [13, 47], we derive the Hamiltonian of the system involving a suitable set of variable for the relevant dipole modes of the circuit, as detailed in the Method and in more details in the Supplementary Note 1. The Hamiltonian of the resulting qubit-qutrit-qubit system shown in Figure 2 takes the form:

$$\begin{aligned}
 H = & \frac{1}{2} \Delta_L \sigma_L^z + \Delta_M |1\rangle \langle 1| + (\Delta_M + \delta_M) |2\rangle \langle 2| + \frac{1}{2} \Delta_R \sigma_R^z \\
 & + J_{LM_{01}} (\sigma_L^- |1\rangle \langle 0| + \sigma_L^+ |0\rangle \langle 1|) \\
 & + J_{RM_{01}} (\sigma_R^- |1\rangle \langle 0| + \sigma_R^+ |0\rangle \langle 1|) \\
 & + J_{LM_{12}} (\sigma_L^- |2\rangle \langle 1| + \sigma_L^+ |1\rangle \langle 2|) \\
 & + J_{RM_{12}} (\sigma_R^- |2\rangle \langle 1| + \sigma_R^+ |1\rangle \langle 2|) \\
 & + J_{LM}^{(z)} \sigma_L^z (D_1 |1\rangle \langle 1| + D_2 |2\rangle \langle 2|) \\
 & + J_{RM}^{(z)} \sigma_R^z (D_1 |1\rangle \langle 1| + D_2 |2\rangle \langle 2|),
 \end{aligned} \tag{1}$$

where σ_α^+ and σ_α^- are the spin-1/2 raising and lowering operators for the left ($\alpha = L$) and right ($\alpha = R$) qubits, σ_α^z is the Pauli Z operator, and $\Delta_{L,R}$ is the energy differences between the spin-up and spin-down states of the corresponding qubit. The states of the qutrit are denoted by $|j\rangle$ ($j = 0, 1, 2$), Δ_M is the energy of state $|1\rangle$

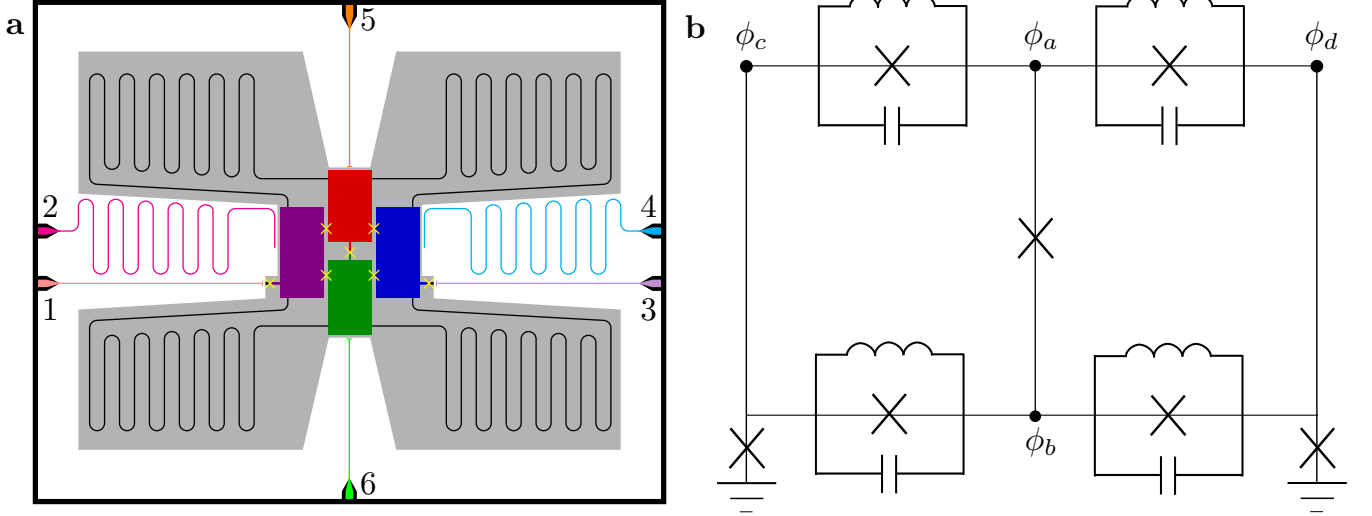


Figure 1. **a** Sketch of a possible physical implementation of the proposed circuit. Each colored box is a superconducting island corresponding to a node in a lumped circuit element model. Josephson junctions are shown schematically as yellow crosses. Bent black wires are inductors. The numbered colored lines are controls for readout and driving of the circuit: 1 and 3 are the flux lines for frequency tuning of the outer qubits, 2 and 4 are resonators capacitively coupled to left and right qubits, and lines 5 and 6 are control and driving of the two middle islands forming the middle qutrit. **b** Effective Lumped circuit scheme of the same circuit. The four nodes in the system are shown as dots and Josephson Junctions are shown as crosses.

and $\Delta_M + \delta_M$ is the energy of state $|2\rangle$, making the anharmonicity equal to $\Delta_M - \delta_M$, with the energy of the ground state $|0\rangle$ set to zero. Δ_M and δ_M can be tuned dynamically by an external flux if additional flux lines are added to the circuit, or by an AC-Stark shift stemming from off-resonant microwave driving [9] using the lines 5 and 6 in fig. 1 (a) (see Supplementary Note 1). We note that the AC-Stark shift is included here for additional dynamical tuning of the circuit but it is not essential for the gate implementations discussed below.

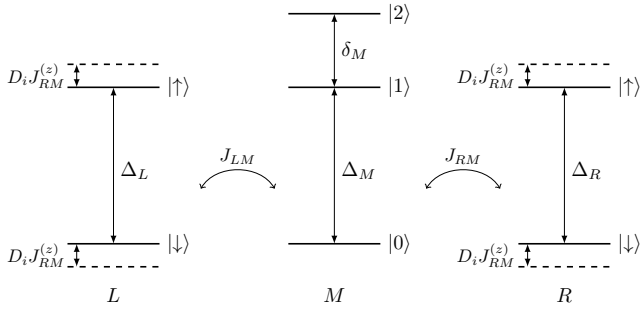


Figure 2. Energy diagram of the system of two qubits (left, L , and right, R) and a qutrit (middle, M) described by the Hamiltonian in Equation (1). Also shown are the exchange couplings $J_{\alpha M}$ and state-dependent energy shifts $J_{\alpha M}^{(z)}$ of $|1\rangle$. D_i depend on the state of the qutrit $|i\rangle$, with, $D_0 = 0$, and typically, $D_1 \gtrsim 2$ and $D_2 \lesssim 4$.

The exchange (XY) coupling strengths between the qubits and the qutrit are given by $J_{\alpha M}$. Typically, the coupling $J_{\alpha M_{12}}$ ($\alpha = L, R$) to the $|1\rangle \leftrightarrow |2\rangle$ transition is stronger than the coupling $J_{\alpha M_{01}}$ to the $|0\rangle \leftrightarrow |1\rangle$ tran-

sition by a factor $\sim \sqrt{2}$. The coefficients $J_{\alpha M}^{(z)}$ determine the dispersive (ZZ) interaction between the qubits and the qutrit with $D_1 \gtrsim 2$ and $D_2 \lesssim 4$, with the two parameters converging at 3 as the mixing is increased via the off-resonant driving. For clarity, these parameters are shown in Figure 2. In a perfectly left-right symmetric circuit, we have $\Delta_L = \Delta_R$ and $J_{LM} = J_{RM}$ for both qutrit transitions which is assumed below unless otherwise stated.

For typical experimental parameters, the coupling strengths J 's are in the range of few to some tenths of MHz, while the energies Δ 's and δ 's are in the 10 GHz range. We choose realistic values of the experimental parameters so as to stay within the transmon regime [13].

Apart from the intrinsic dynamics of the system, we will employ an external microwave (mw) field of (variable) frequency ω_{mw} to drive the system. Physically, the driving can be applied through resonators 2 and 4 capacitively coupled to the outer qubits, and control lines 5 and 6 capacitively coupled to the qutrit, as shown in Figure 1(a). The microwave field induces transitions between the qubit and qutrit states as described by the Hamiltonian

$$H_{mw} = \cos(\omega_{mw}t)(\Omega_L \sigma_L^+ + \Omega_R \sigma_R^+ + \Omega_1 |0\rangle\langle 1| + \Omega_2 |1\rangle\langle 2| + \text{H.c.}), \quad (2)$$

where Ω 's are the corresponding Rabi frequencies. Moreover, multifrequency pulses generated by an appropriate microwave source and directed to the qutrit via the control lines can be used to dynamically tune the qutrit transitions (see Supplementary Note 1 for the general treatment of transitions of a capacitively coupled qutrit).

We note that unlike our qubits and qutrit, in flux qubits optical selection rules may depend on the magnetic flux [48].

Our system can be used to achieve many quantum information tasks, examples of which are described below. The qutrit can encode a qubit in either states $(|0\rangle, |1\rangle)$ or states $(|0\rangle, |2\rangle)$. This is solely a matter of convenience and it is straightforward to toggle between these two encodings by applying a π -pulse on the $|1\rangle \leftrightarrow |2\rangle$ transition.

Qutrit dissociation and entangled state preparation

We now discuss how to deterministically prepare entangled states in the setup, which is of great importance for quantum computation and information tasks [41, 49]. In our system, we can employ the qutrit to deterministically prepare an entangled Bell state between the outer qubits $\frac{1}{\sqrt{2}}(|\downarrow\downarrow\rangle + |\uparrow\uparrow\rangle)$, as detailed below.

First, we tune the energy levels of the qutrit to make its two transitions $|0\rangle \leftrightarrow |1\rangle$ and $|1\rangle \leftrightarrow |2\rangle$ non-resonant with the transitions $|\downarrow\rangle \leftrightarrow |\uparrow\rangle$ of the qubits, i.e., we require that $|\Delta_M - \Delta_\alpha| \gg J_{\alpha M_{01}}$ and $|\delta_M - \Delta_\alpha| \gg J_{\alpha M_{12}}$. Starting from the ground state $|0\rangle$, we produce the superposition state $\frac{1}{\sqrt{2}}(|0\rangle + |2\rangle)$ of the qutrit by external driving, employing the STIRAP (STImulated Raman Adiabatic Passage) sequence of pulses [50], as has been also proposed [51] and implemented [52] in superconducting circuits before. Namely, we drive the transitions $|0\rangle \leftrightarrow |1\rangle$ and $|1\rangle \leftrightarrow |2\rangle$ with resonant mw-pulses of Rabi frequencies Ω_1 and Ω_2 . The Ω_2 pulse precedes the Ω_1 pulse, and we adjust the overlap between the pulses so as to obtain the transfer to state $|2\rangle$ with minimal population of the intermediate state $|1\rangle$. The two pulses are suddenly turned off when their amplitudes are equal, resulting in the desired superposition state. The dynamics of the qutrit under the STIRAP driving is shown in Figure 3 (a), with the inset showing the pulse sequence.

Next, the Bell state is obtained as $\frac{1}{\sqrt{2}}|\downarrow\downarrow\rangle (|0\rangle + |2\rangle) \rightarrow \frac{1}{\sqrt{2}}(|\downarrow\downarrow\rangle + |\uparrow\uparrow\rangle)|0\rangle$ via “dissociation” of the qutrit excitation $|2\rangle$ into two qubit excitations $|\uparrow\uparrow\rangle$. To this end, we set $\Delta_M + \delta_M = \Delta_L + \Delta_R$ and choose $|\Delta_M - \Delta_\alpha| > J_{\alpha M_{01}}$ via tuning the frequencies of the outer qubits with flux control and the qutrit with the dynamical driving. Note that this condition applies when $J_{\alpha M_{01}} = J_{\alpha M_{12}}$. If the exchange coefficients are different, as is normally the case, the qutrit is moved out of the two-photon resonance by unequal second order level shifts $|J_{\alpha M_{01}}|^2/(\Delta_M - \Delta_\alpha) \neq |J_{\alpha M_{12}}|^2/(\delta_M - \Delta_\alpha)$, which can be compensated for by adjusting Δ_M or δ_M . Making the intermediate state $|1\rangle$ non-resonant precludes its population but prolongs the dissociation, which results in a more pronounced effect of the noise and relaxations. The dissociation dynamics $|\downarrow 2 \downarrow\rangle \rightarrow |\uparrow 0 \uparrow\rangle$ is shown in Figure 3.

Using the pairwise ZZ -interactions, the fully entangled three-particle GHZ (Green-Horne-Zeilinger) state $\frac{1}{\sqrt{2}}(|\downarrow 0 \downarrow\rangle + |\uparrow 1 \uparrow\rangle)$ can be obtained from the prepared

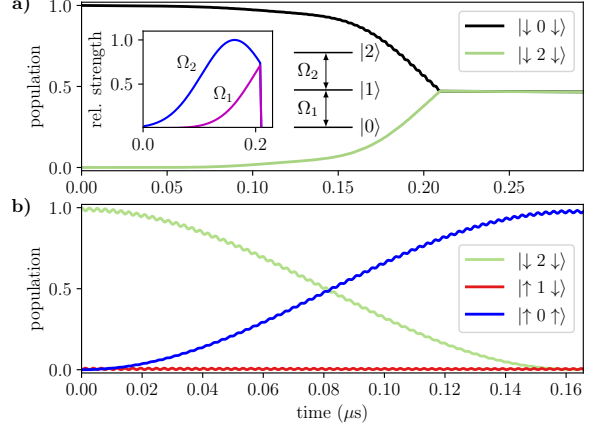


Figure 3. **a)** Populations of states $|0\rangle$, $|1\rangle$ and $|2\rangle$ of the middle qutrit during the half STIRAP in the case of off-resonant qutrit levels and $\max(\Omega_{1,2})/2\pi = 20$ MHz. The inset shows the envelopes of the mw pulses. **b)** Dissociation of the initial state $|\downarrow 2 \downarrow\rangle$ into the final state $|\uparrow 0 \uparrow\rangle$ with the two-photon resonance $\Delta_M + \delta_M = \Delta_L + \Delta_R$ while the intermediate states $|\uparrow 1 \downarrow\rangle$, $|\downarrow 1 \uparrow\rangle$ are off-resonant. We used the parameters $J_{\alpha M_{01}}/2\pi \simeq 15.1$ MHz and $J_{\alpha M_{12}}/2\pi \simeq 19.4$ MHz. We also include finite coherence times as described in Methods.

Bell state $\frac{1}{\sqrt{2}}(|\downarrow 0 \downarrow\rangle + |\uparrow 0 \uparrow\rangle)$ by the external driving of the middle qutrit. To this end, we apply to the circuit a weak π pulse Ω_1 which is resonant only for the $|\uparrow 0 \uparrow\rangle \leftrightarrow |\uparrow 1 \uparrow\rangle$ transition and non-resonant for the $|\downarrow 0 \downarrow\rangle \leftrightarrow |\downarrow 1 \downarrow\rangle$ transition, due to the ZZ interactions with the strengths $J_{\alpha M}^{(z)} \gg \Omega_1$.

Alternatively, we can encode a qubit in the $(|0\rangle, |2\rangle)$ states of the qutrit and produce a different maximally entangled state $\frac{1}{\sqrt{2}}(|\downarrow 2 \downarrow\rangle + |\uparrow 0 \uparrow\rangle)$, equivalent to the GHZ state above. Starting from the simple initial state $|\downarrow 2 \downarrow\rangle$, we use only the intrinsic system dynamics by tuning the parameters until $\Delta_L = \Delta_R = \Delta_M = \delta_M$ and $D_2 J_{\alpha M}^{(z)} = \frac{2\sqrt{6}J_{\alpha M_{01}}}{\sqrt{(n\pi/c_n)^2 - 1}}$ for $n = 1, 2, 3, \dots$ and $c_n = \cos^{-1}\left(\frac{(-1)^{n+1}}{8}\right)$. Here, n is a parameter controlling at which oscillation between the states $|\downarrow 2 \downarrow\rangle$ and $|\uparrow 0 \uparrow\rangle$ their equal superposition is obtained (lower n is quicker). The disadvantage of this scheme is that it requires very precise tuning of the interactions $J_{\alpha M}^{(z)}$. In contrast, for the method above, only the frequencies have to be adjusted, which is easier using the dynamical tuning or an equivalent flux tuning. Further details are given in Supplementary Note 3.

Toffoli and CCZ gates

The controlled-controlled NOT (CCNOT) gate, also called the Toffoli gate, is a reversible and universal 3-bit gate for classical computation [35]. It performs a NOT (bit-flip)

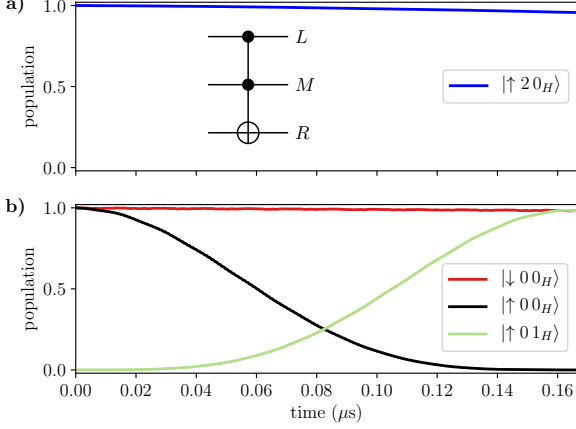


Figure 4. Numerical simulation of the implementation of the CCZ gate in the rotating frame. The phase of the right qubit is flipped, $|0_H\rangle \rightarrow |1_H\rangle$, if the left qubit is in state $|\uparrow\rangle$ and the qutrit is in state $|0\rangle$, otherwise no change occurs as exemplified in a) for the state $|\uparrow 2 0_H\rangle$ and in b) for the state $|\downarrow 0 0_H\rangle$. A subsequent Hadamard gate on the right qubit will yield the desired CCNOT gate. The standard circuit representation of the Toffoli gate is shown as an inset in the upper panel of the figure. See Supplementary Material for the parameters used in the simulation.

operation on the target bit if the two control bits are in state ‘1’, and does nothing otherwise. The Toffoli gate is an important element in many quantum algorithms, such as quantum error correction [53] and Shor’s algorithm [54]. It has been implemented in systems ranging from trapped ions [55] to superconducting circuits [40], including a proposal for an implementation with static control optimized with machine learning [56].

We can implement the CCNOT gate with the left qubit and the middle qutrit acting as controls and the right qubit being the target. The state of the right qubit is then inverted only if the left qubit is in the spin up (excited) state $|\uparrow\rangle$ and the qutrit is in the ground state $|0\rangle$. The second control qubit is encoded in the qutrit states $|0\rangle$ and $|2\rangle$. The quantum CCNOT gate is realized by first executing a double-controlled phase (CCZ) gate that shifts the phase of the state $|\uparrow 0 \uparrow\rangle$ by π (sign change) while nothing happens if either of the outer qubits are in the spin down state or if the qutrit is in state $|2\rangle$. The CCNOT can then be obtained by the transformation: $\text{CCNOT} = \mathcal{H} \cdot \text{CCZ} \cdot \mathcal{H}$, where \mathcal{H} is the Hadamard gate that acts on the target qubit R . In practice, the Hadamard gate can be obtained by a $\pi/2$ rotation about the y axis.

The CCZ gate is implemented by choosing suitable parameters such that the transitions between the qubit and qutrit states are non-resonant, while $J_{\alpha M}^{(z)}$ (> 10 MHz) is large. We apply a weak microwave field on the qutrit transition $|\uparrow 0 \uparrow\rangle \leftrightarrow |\uparrow 1 \uparrow\rangle$ with the Rabi frequency $\Omega_1 \ll J_{\alpha M}^{(z)}$. Because of the ZZ interactions, which yield a state-dependent frequency shift of the qutrit, the mi-

crowave field frequency can be chosen such that it is resonant only when both outer qubits are in the spin-up state. The microwave 2π -pulse then results in the transformation $|0\rangle \rightarrow i|1\rangle \rightarrow -|0\rangle$ that leads to the double conditional π phase change of (only) the state $|\uparrow 0 \uparrow\rangle$. For simplicity, we have here used a standard square-pulse control. In a real-life implementation, a DRAG pulse [57] or similar optimized pulses could be used, suppressing leakage to, and phase errors from, other levels and thus further improving the fidelity. In Figure 4 we show the results of the numerical simulations of the CCZ gate in the Hadamard basis for the right qubit (defined as $|0_H\rangle = |+\rangle = (|\downarrow\rangle + |\uparrow\rangle)/\sqrt{2}$ and $|1_H\rangle = |-\rangle = (|\downarrow\rangle - |\uparrow\rangle)/\sqrt{2}$). Subsequent application of the Hadamard gate to the right qubit will complete the CCNOT gate. We note that because of the symmetry of the driving, we could have also chosen the qutrit state $|1\rangle$ instead of $|0\rangle$ as the ‘open’ state, but here we can view this merely as an ancillary state.

Fredkin gate

Another classically universal 3-bit gate is the Fredkin gate, whose quantum analog is the controlled SWAP (CSWAP) gate. Its effect is to swap the states of the two qubits, $|\uparrow\downarrow\rangle \leftrightarrow |\downarrow\uparrow\rangle$, conditional upon the state of a control qubit, here encoded in the qutrit. We now use the two lowest states ($|0\rangle$ and $|1\rangle$) of the qutrit to encode the qubit such that the excited state $|1\rangle$ is ‘on’ and the ground state $|0\rangle$ is ‘off’. To realize CSWAP, we tune the energy levels of the qutrit such that the transition $|1\rangle \leftrightarrow |2\rangle$ is resonant with the qubit transitions $|\uparrow\rangle \leftrightarrow |\downarrow\rangle$, i.e. $\Delta_L \simeq \delta_M \simeq \Delta_R$. Simultaneously, the qutrit transition $|0\rangle \leftrightarrow |1\rangle$ is largely detuned, $|\Delta_M - \Delta_{L,R}| \gg J_{\alpha M_{01}}$. We then keep the resonance of the exchange interaction $J_{\alpha M_{12}} \gg J_{\alpha M}^{(z)}$ for time $T = \pi/\sqrt{2}J_{\alpha M_{12}}$. If the qutrit is in state $|0\rangle$, the qubits remain in their initial states due to absence of resonant transitions. But if the qutrit is in state $|1\rangle$, it would induce the swap between the qubit states, $|\uparrow 1 \downarrow\rangle \leftrightarrow |\downarrow 1 \uparrow\rangle$, via the resonant intermediate state $|\downarrow 2 \downarrow\rangle$ involving the qutrit excitation. (Resonant swap between the qubits would also occur for the qutrit initially in state $|2\rangle$, with the intermediate state being $|\uparrow 1 \uparrow\rangle$.) This is illustrated in Figure 5 (a).

As can also be seen in Figure 5 (a), however, the initial state $|\downarrow 1 \downarrow\rangle$ has trivial dynamics, unlike the rest of the swapped states which attain a π phase shift during the interaction time T . This means that we have a SWAP operation only up to a conditional phase for an arbitrary superposition input state. This is related to the phase shift of the swapped terms arising in the iSWAP gate, obtained by directly coupling two resonant qubits, which has recently attracted great interest [9, 58]. In our case with the qutrit mediating the swap, only one state has a sign that needs correction, similarly to what Kivlichan et al. has recently called the “fermionic simulation gate” [59]. Because of this, we can easily mitigate this problem

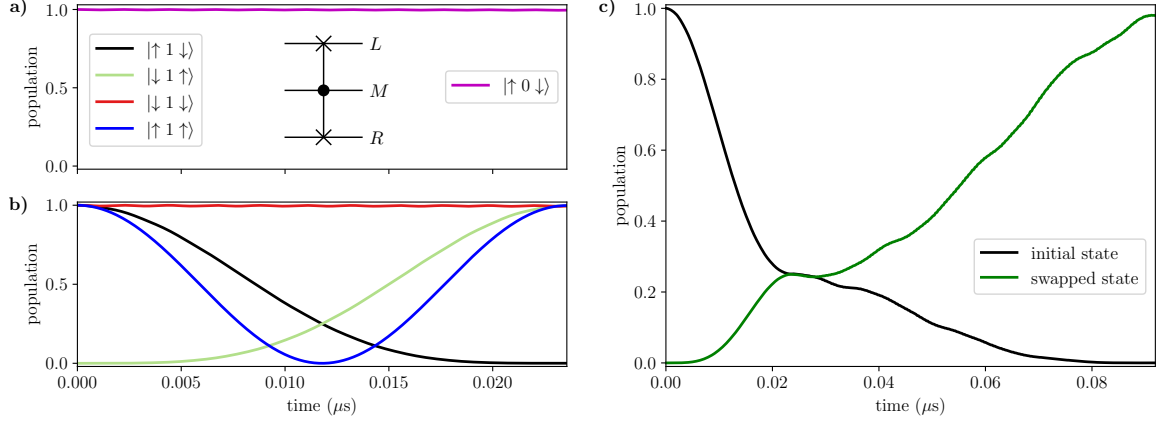


Figure 5. **a)** and **b)** Numerical simulations of the ACSWAP (almost CSWAP) gate for different computational basis states, with the exchange interaction $J_{\alpha M_{12}}$ resonant for time $T = \pi/\sqrt{2J_{\alpha M_{12}}}$. The standard circuit representation of the Fredkin gate is shown as an inset in the top part of the figure. **b)** Numerical simulation of the full CSWAP gate for the initial superposition state $[\cos(\theta_1)|\uparrow\rangle + e^{i\phi_1}\sin(\theta_1)|\downarrow\rangle]|1\rangle[\cos(\theta_2)|\uparrow\rangle + e^{i\phi_2}\sin(\theta_2)|\downarrow\rangle]$ with $\theta_1 = \pi/4$, $\phi_1 = 3\pi/4$, $\theta_2 = 3\pi/4$ and $\phi_2 = \phi_1$. In part 1, we perform the ACSWAP operation during time $T_1 = \pi/2J_{\alpha M_{01}}$ with the parameters as in figure 5. In part 2 we perform the CCZ gate during time $T_2 = 2\pi/\Omega_2$ with the resonant mw field of frequency $\omega_{mw} = \delta_M - 2J_{\alpha M}^{(z)}$. The full CSWAP fidelity of this state is > 0.98 , with finite coherence times included. See Supplementary Material for the parameters used in the simulation.

by using the CCZ gate (see Subsection “Toffoli and CCZ gates”) to attain the π phase shift of state $|\downarrow 1 \downarrow\rangle$ and obtain the correct CSWAP gate. In Figure 5 (b) we show the results of our numerical simulations of the complete CSWAP protocol, including the conditional resonant SWAP followed by the CCZ gate with a total fidelity $> 98\%$. More detailed analysis is given in Supplementary Note 4.

We note that we could have equivalently performed the CSWAP gate between the two qubits via the resonant qutrit transition $|0\rangle \leftrightarrow |1\rangle$, while the other transition $|1\rangle \leftrightarrow |2\rangle$ is non-resonant. In our scheme, the qutrit has to play the role of control and thus our Fredkin gate is not a universal multi-qubit gate in itself. We could, however, imagine another qubit with controlled coupling to the qutrit as part of a larger universal circuit.

Double-controlled holonomic gate

Another concept with importance to quantum computation [34] is the implementation of general (non-abelian) one-qubit gates of the form (neglecting overall phase factors)

$$U = \begin{pmatrix} e^{i\phi_1} \cos(\theta) & e^{i\phi_2} \sin(\theta) \\ -e^{-i\phi_2} \sin(\theta) & e^{-i\phi_1} \cos(\theta) \end{pmatrix}. \quad (3)$$

Together with a non-trivial (entangling) multi-qubit gate, they form a universal set of quantum gates [34]. We can implement the non-adiabatic one-qubit holonomic gate [44, 60] with our qutrit, choosing states $(|0\rangle, |2\rangle)$ to encode the qubit. Such gates have the advantages of being robust to parameter fluctuations due to the geometric nature, without the limitations of long gate operation times

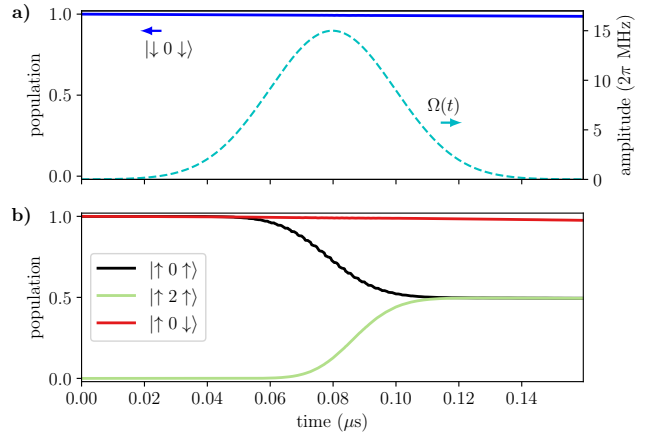


Figure 6. **a)** and **b)** Populations (left vertical axes) as function of time during the operation of the controlled-controlled holonomic gate in the case of $\theta = \pi/4$ and $\phi = 0$. Panel **a)** also shows the envelope of the external fields plotted with dotted lines with the corresponding vertical axis on the right of the plot. See Supplementary Material for the parameters used in the simulation.

required to satisfy the adiabatic requirement [61, 62]. Holonomic gates have been implemented in a range of different systems [63, 64], and their stability has been well tested [65, 66]. Choosing the same system parameters as for the CCZ gate above, we use a driving scheme inspired by [63] and thereby realize the single-qubit gate

$$U(\phi, \theta) = \begin{pmatrix} \cos(\theta) & e^{i\phi} \sin(\theta) \\ e^{-i\phi} \sin(\theta) & -\cos(\theta) \end{pmatrix}, \quad (4)$$

with the computational qubit states as basis. This transformation is less general than (3), but it is still universal for one-qubit rotations.

We drive the two transitions $|0\rangle \leftrightarrow |1\rangle$ and $|1\rangle \leftrightarrow |2\rangle$ with the external fields having the same Gaussian envelope $\Omega(t)$ but different complex coupling amplitudes a and b , i.e. $\Omega_1(t) = a\Omega(t)$ and $\Omega_2(t) = b\Omega(t)$ in Equation (2), satisfying $|a|^2 + |b|^2 = 1$. The pulse $\Omega(t)$ is turned on at time $t = 0$ and turned off at $t = \tau$, such that we get a 2π -pulse, $\int_0^\tau \Omega(t)dt = 2\pi$. Notice that this condition ensures that we end up with a closed path in parameter space and the gate is indeed holonomic. Starting with the qutrit in the ground state $|0\rangle$, we then obtain the final transformation $U(\phi, \theta)$ of Equation (4) acting on the qutrit states $|0\rangle, |2\rangle$. Here θ and ϕ are defined via $e^{i\phi} \tan(\theta/2) = a/b$.

By using the $J_{\alpha M}^{(z)}$ couplings to shift the qutrit frequencies, we can make the external driving field resonant or not, depending on the states of the outer qubits. This condition would then result in a controlled-controlled holonomic gate transforming the state of the qutrit according to (4) only when the outer (control) qubits are in e.g. the spin up state. We can show that this new gate is universal for quantum computing by first writing it in the three-qubit computational basis with $|6\rangle = |\uparrow 0 \uparrow\rangle$ and $|7\rangle = |\uparrow 2 \uparrow\rangle$, and the rest of the 8 basis states numbered from 0 to 5:

$$U^c(\phi, \theta) = \left(\begin{array}{c|cc} \mathbb{I} & 0 \\ \hline 0 & \cos(\theta) & e^{i\phi} \sin(\theta) \\ & e^{-i\phi} \sin(\theta) & -\cos(\theta) \end{array} \right), \quad (5)$$

where \mathbb{I} is the 6×6 identity matrix and the superscript c indicates that this is the controlled version of the holonomic gate. We now apply this transformation twice:

$$U^c(\pi/2, \theta)U^c(0, 0) = \left(\begin{array}{c|cc} \mathbb{I} & 0 \\ \hline 0 & \cos(\theta) & -i \sin(\theta) \\ & -i \sin(\theta) & \cos(\theta) \end{array} \right). \quad (6)$$

This is equal to the famous Deutsch gate except for a factor i on the 2×2 rotation matrix. The Deutsch gate is universal for quantum computation [67], and thus our double-controlled holonomic gate is also universal. Implementation of this gate have previously been proposed using Rydberg atoms [68], albeit using three laser pulses instead of only two as in our case.

In Figure 6 we show the evolution of different initial states under gate operation. Evidently, the qutrit rotation is blocked when the left qubit is in the spin-down state or both qubits are in the spin down state while the qutrit is rotated according to Equation (4) when both qubits are in the excited state.

In Figure 7, we show the populations of the final states for various values of θ , while $\phi = 0$. The theoretical curves $\cos^2\theta$ and $\sin^2\theta$ from (4) are also shown and we observe a very good agreement. The final population of the blocked state $|\downarrow 0 \uparrow\rangle$ is somewhat lower than expected primarily due to leakage to the other levels via a weak interaction with the external field, even though it is far

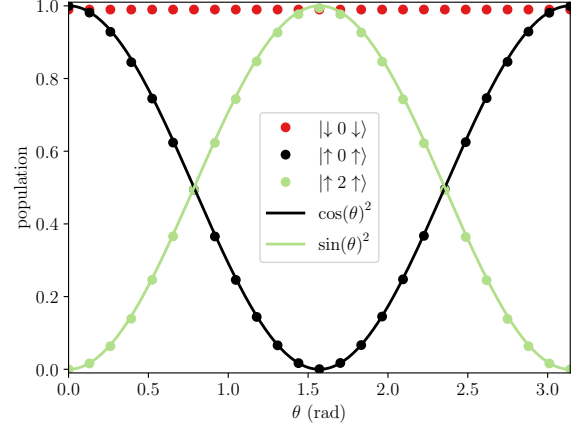


Figure 7. Populations of state versus θ ($\phi = 0$) after the application of the controlled-controlled holonomic gate to the initial state $|\uparrow 0 \uparrow\rangle$ (black and green points) and $|\downarrow 0 \uparrow\rangle$ (red points). See Supplementary Material for the parameters used in the simulation.

from resonance. This leakage is also apparent in Figure 6 and can potentially be reduced by employing pulse shaping techniques [57].

DISCUSSION

To summarize, we have proposed a realistic superconducting circuit, consisting of a qutrit and two qubits, for efficient implementations of multi-qubit quantum gates. By utilizing the second excited state of the qutrit in the middle position, we proposed simple schemes for generating a maximally entangled Bell state of the outer qubits and a GHZ state of the qubits and the qutrit. Furthermore, our construction can implement several important quantum gates, such as the CCNOT (Toffoli), and CSWAP (Fredkin) gates. We note that with qubits only, the theoretically most efficient realizations of the Fredkin and Toffoli gates each requires five two-qubit gates [38]. State of the art implementations of the Toffoli and CCZ gates using superconducting circuits have operation times ranging from 90 ns (with poor fidelity) [40] to about 260 ns [69]. As for the Fredkin gate, we are not aware of an implementation with a superconducting circuit, but a hybrid scheme proposal has a gate execution time of 350 ns [70]. Using the current state of the art superconducting systems requiring 40 ns per two-qubit gate [71, 72], the total three-qubit gate time would be at least 200 ns. For comparison, our proposed scheme can complete the three-qubit operations in 100 ns. Thus, our results exemplify the flexibility and usefulness of qutrits for very efficient realizations of three-qubit gates, and demonstrate the potential of our circuit to serve as a basis for more complicated superconducting circuits.

Our scheme can implement in principle any controlled-

controlled unitary operation on the qutrit. As an example, we have considered the double-controlled non-abelian holonomic quantum gate on a single qubit, which can be used to implement the three-qubit Deutsch gate in only two operations. This implementation is more effective than current proposals with Rydberg atoms [68], while we are not aware of an implementation using superconducting circuits. We have implemented the holonomic gate as it is robust to parameter noise [61] stemming from the geometric nature of this gate. The strategy of using such gates is known as holonomic quantum computation (HQC) [44] and the universal non-abelian HQC (NHQC) generalization has since been performed by Sjöqvist et al. [46]. Here, three bare energy eigenstates are needed and are conveniently provided by the qutrit. A natural next step is to try to implement the two-qubit non-adiabatic holonomic quantum gate also suggested by Sjöqvist et al., requiring two nearest-neighbor qutrits. Such a gate could be possibly achieved by our circuit upon expanding the basis of one of the outer qubits. Together with the holonomic one-qubit gate, this would realize a universal set of holonomic gates.

Realizing qutrit-qutrit interactions would also open the possibility of implementing higher-order effective spin chains, such as the spin-one Haldane spin model [73, 74], especially if the coherence times of higher levels are further prolonged [75].

Another possible use of qutrits and a circuit similar to the one proposed in this paper is the implementation of autonomous quantum error correction via engineered dissipation. With a relatively small increase in circuit complexity including three energy levels, an impressive increase in transmon coherence time was predicted in Ref. [76].

METHODS

Consider the circuit with four connected superconducting islands with lumped element circuit shown in Figure 1 (b). After obtaining the Lagrangian of the corresponding effective lumped element model system in the node flux picture, we perform a suitable change of coordinates, primarily mixing the two central flux node coordinates: $\psi_1 = \phi_a + \phi_b - 2\phi_c$, $\psi_2 = \phi_a - \phi_b$ and $\psi_3 = \phi_a + \phi_b - 2\phi_d$, where the ϕ s are the flux node variables shown in the circuit (in natural units). They represent the horizontal dipole mode between the left superconducting island and the two middle islands, the vertical dipole mode between the two middle islands, and the horizontal mode between the right island and the two middle islands, respectively. With this choice of coordinates, we obtain three effective nodes with the relevant degrees of freedom sequentially coupled via non-linear interactions. We truncate the outer nodes to the lowest two states, obtaining qubits, while for the middle node we instead choose to truncate its Hilbert space to the lowest three energy lev-

els, obtaining a qutrit. All three degrees of freedom are in the transmon limit with the kinetic energy terms being much smaller than the potential energy terms. Finally, by transforming to a rotating frame and making a rotating wave approximation to eliminate the fast oscillating terms, we obtain an effective Hamiltonian for the system of two qubits each coupled to the qutrit (see Supplementary Note 1 for the full derivation). This Hamiltonian is given in (1).

The drive line terms are added to the non-truncated Lagrangian as externally varied flux nodes and a transformation to an appropriate frame rotating with the external field is performed. This transformation mixes the variables and after additional rotating wave approximations, the desired external part of the Hamiltonian is obtained along with modifications on the energy parameters, i.e. the AC-Stark shifts, which can be used for tuning the qubits and qutrit in and out of resonance.

We simulate the dissipative dynamics of the system numerically, with the relaxation and decoherence times set to $T_1 = 31 \mu\text{s}$ and $T_2 = 35 \mu\text{s}$ respectively, based on recent studies [15, 75, 77] (we use the Python QuTip package [78], and relaxations are implemented by the simple built-in collapse operator functionality). The parameters of the Hamiltonian used in the numerical simulations are all obtained from realistic experimental circuit parameters, as detailed in Supplementary Note 1, and are listed in Supplementary Note 2 for each implementation.

Data availability

The data that support the findings of this study are available from N.T.Z. upon request.

ACKNOWLEDGMENTS

We thank W. D. Oliver, S. Gustavsson, and M. Kjaergaard from the Engineering Quantum Systems Group at MIT for their kind hospitality and for extended discussion on superconducting circuits. This work was supported by the Carlsberg Foundation and the Danish Council for Independent Research under the DFF Sapere Aude program.

Author contributions

The circuit was designed by L.B.K. and N.J.S.L., and analyzed by L.B.K. and T.B. The numerical calculations were performed by T.B. with suggestions from D.P., C.K.A., N.J.S.L. and N.T.Z. The initial draft of the paper was written by T.B., D.P. and N.T.Z. All authors contributed to the revisions that lead to the final version.

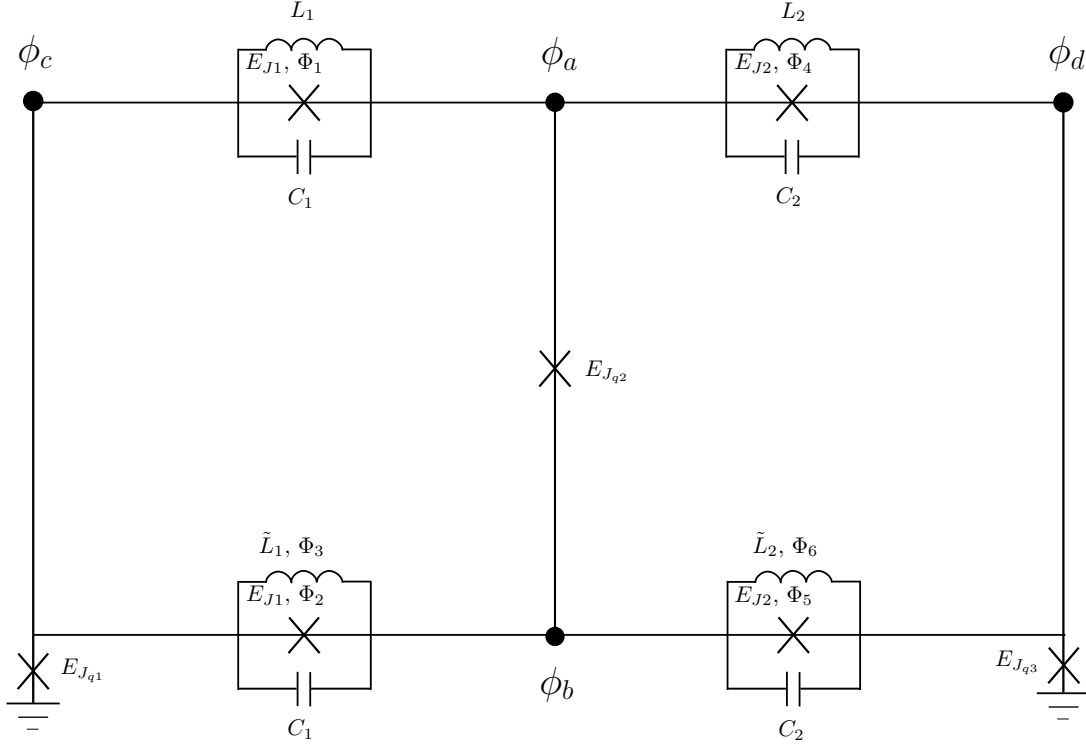
-
- [1] R. P. Feynman, “Simulating physics with computers,” *International Journal of Theoretical Physics* **21**, 467–488 (1982).
- [2] S. Lloyd, “Universal quantum simulators,” *Science* **273**, 1073–1078 (1996).
- [3] D. Porras and J. I. Cirac, “Effective quantum spin systems with trapped ions,” *Phys. Rev. Lett.* **92**, 207901 (2004).
- [4] R. Blatt and C. F. Roos, “Quantum simulations with trapped ions,” *Nature Physics* **8**, 277 (2012), review Article.
- [5] A. A. Khajetoorians, J. Wiebe, B. Chilian, and R. Wiesendanger, “Realizing all-spin-based logic operations atom by atom,” *Science* **332**, 1062–1064 (2011).
- [6] F. A. Zwanenburg, A. S. Dzurak, A. Morello, M. Y. Simmons, L. C. L. Hollenberg, G. Klimeck, S. Rogge, S. N. Coppersmith, and M. A. Eriksson, “Silicon quantum electronics,” *Rev. Mod. Phys.* **85**, 961–1019 (2013).
- [7] A. Blais, J. Gambetta, A. Wallraff, D. I. Schuster, S. M. Girvin, M. H. Devoret, and R. J. Schoelkopf, “Quantum-information processing with circuit quantum electrodynamics,” *Phys. Rev. A* **75**, 032329 (2007).
- [8] John M. Martinis, S. Nam, J. Aumentado, and C. Urbina, “Rabi oscillations in a large josephson-junction qubit,” *Phys. Rev. Lett.* **89**, 117901 (2002).
- [9] A. Blais, R.-S. Huang, A. Wallraff, S. M. Girvin, and R. J. Schoelkopf, “Cavity quantum electrodynamics for superconducting electrical circuits: An architecture for quantum computation,” *Phys. Rev. A* **69**, 062320 (2004).
- [10] M. H. Devoret and R. J. Schoelkopf, “Superconducting circuits for quantum information: An outlook,” *Science* **339**, 1169–1174 (2013).
- [11] G. Wendin, “Quantum information processing with superconducting circuits: a review,” *Reports on Progress in Physics* **80**, 106001 (2017).
- [12] Xiu Gu, Anton Frisk Kockum, Adam Miranowicz, Yu xi Liu, and Franco Nori, “Microwave photonics with superconducting quantum circuits,” *Physics Reports* **718-719**, 1 – 102 (2017).
- [13] J. Koch, T. M. Yu, J. Gambetta, A. A. Houck, D. I. Schuster, J. Majer, A. Blais, M. H. Devoret, S. M. Girvin, and R. J. Schoelkopf, “Charge-insensitive qubit design derived from the Cooper pair box,” *Phys. Rev. A* **76**, 042319 (2007).
- [14] R. Barends, J. Kelly, A. Megrant, D. Sank, E. Jeffrey, Y. Chen, Y. Yin, B. Chiaro, J. Mutus, C. Neill, P. O’Malley, P. Roushan, J. Wenner, T. C. White, A. N. Cleland, and John M. Martinis, “Coherent josephson qubit suitable for scalable quantum integrated circuits,” *Phys. Rev. Lett.* **111**, 080502 (2013).
- [15] C. Rigetti, J. M. Gambetta, S. Poletto, B. L. T. Plourde, J. M. Chow, A. D. Córcoles, J. A. Smolin, S. T. Merkel, J. R. Rozen, G. A. Keefe, M. B. Rothwell, M. B. Ketchen, and M. Steffen, “Superconducting qubit in a waveguide cavity with a coherence time approaching 0.1 ms,” *Phys. Rev. B* **86**, 100506 (2012).
- [16] A. Kandala, A. Mezzacapo, K. Temme, M. Takita, M. Brink, J. M. Chow, and J. M. Gambetta, “Hardware-efficient variational quantum eigensolver for small molecules and quantum magnets,” *Nature* **549**, 242–246 (2017).
- [17] Z. Wang, S. Shankar, Z. K. Mineev, P. Campagne-Ibarcq, A. Narla, and M. H. Devoret, “Cavity Attenuators for Superconducting Qubits,” *ArXiv e-prints* (2018), arXiv:1807.04849 [quant-ph].
- [18] Austin G. Fowler, Matteo Mariantoni, John M. Martinis, and Andrew N. Cleland, “Surface codes: Towards practical large-scale quantum computation,” *Phys. Rev. A* **86**, 032324 (2012).
- [19] R. Barends, J. Kelly, A. Megrant, A. Veitia, D. Sank, E. Jeffrey, T. C. White, J. Mutus, A. G. Fowler, B. Campbell, Y. Chen, Z. Chen, B. Chiaro, A. Dunsworth, C. Neill, P. O’Malley, P. Roushan, A. Vainsencher, J. Wenner, A. N. Korotkov, A. N. Cleland, and John M. Martinis, “Superconducting quantum circuits at the surface code threshold for fault tolerance,” *Nature* **508**, 500–503 (2014).
- [20] T. Yamamoto, Yu A. Pashkin, O. Astafiev, Y. Nakamura, and J. S. Tsai, “Demonstration of conditional gate operation using superconducting charge qubits,” *Nature* **425**, 941 (2003).
- [21] L. DiCarlo, J. M. Chow, J. M. Gambetta, Lev S. Bishop, B. R. Johnson, D. I. Schuster, J. Majer, A. Blais, L. Frunzio, S. M. Girvin, and R. J. Schoelkopf, “Demonstration of two-qubit algorithms with a superconducting quantum processor,” *Nature* **460**, 240 (2009).
- [22] Yu Chen, C. Neill, P. Roushan, N. Leung, M. Fang, R. Barends, J. Kelly, B. Campbell, Z. Chen, B. Chiaro, A. Dunsworth, E. Jeffrey, A. Megrant, J. Y. Mutus, P. J. J. O’Malley, C. M. Quintana, D. Sank, A. Vainsencher, J. Wenner, T. C. White, Michael R. Geller, A. N. Cleland, and John M. Martinis, “Qubit architecture with high coherence and fast tunable coupling,” *Phys. Rev. Lett.* **113**, 220502 (2014).
- [23] David C. McKay, Stefan Filipp, Antonio Mezzacapo, Easwar Magesan, Jerry M. Chow, and Jay M. Gambetta, “Universal gate for fixed-frequency qubits via a tunable bus,” *Phys. Rev. Applied* **6**, 064007 (2016).
- [24] Chao Song, Kai Xu, Wuxin Liu, Chui-ping Yang, Shi-Biao Zheng, Hui Deng, Qiwei Xie, Keqiang Huang, Qiu-jiang Guo, Libo Zhang, Pengfei Zhang, Da Xu, Dongning Zheng, Xiaobo Zhu, H. Wang, Y.-A. Chen, C.-Y. Lu, Siyuan Han, and Jian-Wei Pan, “10-qubit entanglement and parallel logic operations with a superconducting circuit,” *Phys. Rev. Lett.* **119**, 180511 (2017).
- [25] Sarah Sheldon, Easwar Magesan, Jerry M. Chow, and Jay M. Gambetta, “Procedure for systematically tuning up cross-talk in the cross-resonance gate,” *Phys. Rev. A* **93**, 060302 (2016).
- [26] Matthew Reagor, Christopher B. Osborn, Nikolas Tezak, Alexa Staley, Guenevere Prawiroatmodjo, Michael Scheer, Nasser Alidoust, Eyob A. Sete, Nicolas Didier, Marcus P. da Silva, Ezer Acala, Joel Angeles, Andrew Bestwick, Maxwell Block, Benjamin Bloom, Adam Bradley, Catvu Bui, Shane Caldwell, Lauren Capelluto, Rick Chilcott, Jeff Cordova, Genya Crossman, Michael Curtis, Saniya Deshpande, Tristan El Bouayadi, Daniel Girshovich, Sabrina Hong, Alex Hudson, Peter Karalekas, Kat Kuang, Michael Lenihan, Riccardo Marenti, Thomas Manning, Jayss Marshall, Yuvraj Mohan, William O’Brien, Johannes Otterbach, Alexander Papageorge, Jean-Philip Paquette, Michael Pel-

- string, Anthony Polloreno, Vijay Rawat, Colm A. Ryan, Russ Renzas, Nick Rubin, Damon Russel, Michael Rust, Diego Scarabelli, Michael Selvanayagam, Rodney Sinclair, Robert Smith, Mark Suska, Ting-Wai To, Mehrnoosh Vahidpour, Nagesh Vodrahalli, Tyler Whyland, Kamal Yadav, William Zeng, and Chad T. Rigetti, “Demonstration of universal parametric entangling gates on a multi-qubit lattice,” *Science Advances* **4** (2018), 10.1126/sciadv.aao3603.
- [27] Matthew Neeley, Radoslaw C. Bialczak, M. Lenander, E. Lucero, Matteo Mariantoni, A. D. O’Connell, D. Sank, H. Wang, M. Weides, J. Wenner, Y. Yin, T. Yamamoto, A. N. Cleland, and John M. Martinis, “Generation of three-qubit entangled states using superconducting phase qubits,” *Nature* **467**, 570 (2010).
- [28] Xiang-Bin Wang, J. Q. You, and Franco Nori, “Quantum entanglement via two-qubit quantum Zeno dynamics,” *Phys. Rev. A* **77**, 062339 (2008).
- [29] G. Romero, D. Ballester, Y. M. Wang, V. Scarani, and E. Solano, “Ultrafast quantum gates in circuit QED,” *Phys. Rev. Lett.* **108**, 120501 (2012).
- [30] Yimin Wang, Jiang Zhang, Chunfeng Wu, J. Q. You, and G. Romero, “Holonomic quantum computation in the ultrastrong-coupling regime of circuit QED,” *Phys. Rev. A* **94**, 012328 (2016).
- [31] Shruti Puri and Alexandre Blais, “High-fidelity resonator-induced phase gate with single-mode squeezing,” *Phys. Rev. Lett.* **116**, 180501 (2016).
- [32] Christian Kraglund Andersen and Klaus Mølmer, “Multifrequency modes in superconducting resonators: Bridging frequency gaps in off-resonant couplings,” *Phys. Rev. A* **91**, 023828 (2015).
- [33] Baptiste Royer, Arne L. Grimsmo, Nicolas Didier, and Alexandre Blais, “Fast and high-fidelity entangling gate through parametrically modulated longitudinal coupling,” *Quantum* **1**, 11 (2017).
- [34] M. A. Nielsen and I. L. Chuang, *Quantum Computation and Quantum Information: 10th Anniversary Edition* (Cambridge University Press, Cambridge, 2010).
- [35] T. Toffoli, “Reversible computing,” in *Automata, Languages and Programming: Seventh Colloquium Noordwijkerhout, the Netherlands July 14–18, 1980*, edited by Jaco de Bakker and Jan van Leeuwen (Springer Berlin Heidelberg, Berlin, Heidelberg, 1980) pp. 632–644.
- [36] E. Fredkin and T. Toffoli, “Conservative logic,” *International Journal of Theoretical Physics* **21**, 219–253 (1982).
- [37] N. Yu and M. Ying, “Optimal simulation of Deutsch gates and the Fredkin gate,” *Phys. Rev. A* **91**, 032302 (2015).
- [38] N. Yu, R. Duan, and M. Ying, “Five two-qubit gates are necessary for implementing the Toffoli gate,” *Phys. Rev. A* **88**, 010304 (2013).
- [39] B. P. Lanyon, M. Barbieri, M. P. Almeida, T. Jennewein, T. C. Ralph, K. J. Resch, G. J. Pryde, J. L. O’Brien, A. Gilchrist, and A. G. White, “Simplifying quantum logic using higher-dimensional Hilbert spaces,” *Nature Physics* **5**, 134–140 (2008).
- [40] A. Fedorov, L. Steffen, M. Baur, M. P. da Silva, and A. Wallraff, “Implementation of a toffoli gate with superconducting circuits,” *Nature* **481**, 170–172 (2012).
- [41] R. Jozsa, “Entanglement and quantum computation,” in *Geometric Issues in the Foundations of Science*, edited by S. Huggett, L. Mason, K. P. Tod, S. T. Tsou, and N. M. J. Woodhouse (Oxford University Press, Oxford, 1997).
- [42] L. DiCarlo, M. D. Reed, L. Sun, B. R. Johnson, J. M. Chow, J. M. Gambetta, L. Frunzio, S. M. Girvin, M. H. Devoret, and R. J. Schoelkopf, “Preparation and measurement of three-qubit entanglement in a superconducting circuit,” *Nature* **467**, 574–578 (2010).
- [43] L.-M. Duan, J. I. Cirac, and P. Zoller, “Geometric manipulation of trapped ions for quantum computation,” *Science* **292**, 1695–1697 (2001).
- [44] P. Zanardi and M. Rasetti, “Holonomic quantum computation,” *Physics Letters A* **264**, 94 – 99 (1999).
- [45] L.-A. Wu, P. Zanardi, and D. A. Lidar, “Holonomic quantum computation in decoherence-free subspaces,” *Phys. Rev. Lett.* **95**, 130501 (2005).
- [46] E. Sjöqvist, D. M. Tong, L. M. Andersson, B. Hessmo, M. Johansson, and K. Singh, “Non-adiabatic holonomic quantum computation,” *New Journal of Physics* **14**, 103035 (2012).
- [47] M. H. Devoret, “Quantum fluctuations in electrical circuits,” in *Les Houches, Session LXIII 7.8* (Elsevier Science B.V., Amsterdam, 1997).
- [48] Yu-xi Liu, J. Q. You, L. F. Wei, C. P. Sun, and Franco Nori, “Optical selection rules and phase-dependent adiabatic state control in a superconducting quantum circuit,” *Phys. Rev. Lett.* **95**, 087001 (2005).
- [49] D. P. DiVincenzo, “The physical implementation of quantum computation,” *Fortschritte der Physik* **48**, 771 (2000).
- [50] N. V. Vitanov, A. A. Rangelov, B. W. Shore, and K. Bergmann, “Stimulated Raman adiabatic passage in physics, chemistry and beyond,” *Rev. Mod. Phys.* **89** (2017), 10.1103/RevModPhys.89.015006.
- [51] L. F. Wei, J. R. Johansson, L. X. Cen, S. Ashhab, and Franco Nori, “Controllable coherent population transfers in superconducting qubits for quantum computing,” *Phys. Rev. Lett.* **100**, 113601 (2008).
- [52] K. S. Kumar, A. Vepsäläinen, S. Danilin, and G. S. Paraoanu, “Stimulated Raman adiabatic passage in a three-level superconducting circuit,” *Nature Communications* **7**, 10628 (2016).
- [53] D. G. Cory, M. D. Price, W. Maas, E. Knill, R. Laflamme, W. H. Zurek, T. F. Havel, and S. S. Somaroo, “Experimental quantum error correction,” *Phys. Rev. Lett.* **81**, 2152–2155 (1998).
- [54] P. W. Shor, “Polynomial-time algorithms for prime factorization and discrete logarithms on a quantum computer,” *SIAM Journal on Computing* **26**, 1484–1509 (1997).
- [55] T. Monz, K. Kim, W. Hänsel, M. Riebe, A. S. Villar, P. Schindler, M. Chwalla, M. Hennrich, and R. Blatt, “Realization of the quantum Toffoli gate with trapped ions,” *Phys. Rev. Lett.* **102**, 040501 (2009).
- [56] L. Banchi, N. Pancotti, and S. Bose, “Quantum gate learning in qubit networks: Toffoli gate without time-dependent control,” *npj Quantum Information* **2**, 16019 (2016).
- [57] F. Motzoi, J. M. Gambetta, P. Rebentrost, and F. K. Wilhelm, “Simple pulses for elimination of leakage in weakly nonlinear qubits,” *Phys. Rev. Lett.* **103**, 110501 (2009).
- [58] Marco Roth, Marc Ganzhorn, Nikolaj Moll, Stefan Filipp, Gian Salis, and Sebastian Schmidt, “Analysis of a parametrically driven exchange-type gate and a two-photon excitation gate between superconducting qubits,”

- Phys. Rev. A **96**, 062323 (2017).
- [59] Ian D. Kivlichan, Jarrod McClean, Nathan Wiebe, Craig Gidney, Alán Aspuru-Guzik, Garnet Kin-Lic Chan, and Ryan Babbush, “Quantum simulation of electronic structure with linear depth and connectivity,” *Phys. Rev. Lett.* **120**, 110501 (2018).
 - [60] J. K. Pachos, *Introduction to Topological Quantum Computation*, 1st ed. (Cambridge University Press, New York, 2012).
 - [61] P. Solinas, P. Zanardi, and N. Zanghì, “Robustness of non-abelian holonomic quantum gates against parametric noise,” *Phys. Rev. A* **70**, 042316 (2004).
 - [62] J. Pachos and P. Zanardi, “quantum holonomies for quantum computing,” *International Journal of Modern Physics B* **15**, 1257–1285 (2001).
 - [63] A. A. Abdumalikov Jr, J. M. Fink, K. Juliusson, M. Pechal, S. Berger, A. Wallraff, and S. Filipp, “Experimental realization of non-abelian non-adiabatic geometric gates,” *Nature* **496**, 482–485 (2013).
 - [64] G. Feng, G. Xu, and G. Long, “Experimental realization of nonadiabatic holonomic quantum computation,” *Phys. Rev. Lett.* **110**, 190501 (2013).
 - [65] S. Filipp, J. Klepp, Y. Hasegawa, C. Plonka-Spehr, U. Schmidt, P. Geltenbort, and H. Rauch, “Experimental demonstration of the stability of Berry’s phase for a spin-1/2 particle,” *Phys. Rev. Lett.* **102**, 030404 (2009).
 - [66] J. C. Loredó, M. A. Broome, D. H. Smith, and A. G. White, “Observation of entanglement-dependent two-particle holonomic phase,” *Phys. Rev. Lett.* **112**, 143603 (2014).
 - [67] David Deutsch, “Quantum computational networks,” *Proceedings of the Royal Society of London A: Mathematical, Physical and Engineering Sciences* **425**, 73–90 (1989).
 - [68] Xiao-Feng Shi, “Deutsch, Toffoli, and cnot gates via Rydberg blockade of neutral atoms,” *Phys. Rev. Applied* **9**, 051001 (2018).
 - [69] Edwin Barnes, Christian Arenz, Alexander Pitchford, and Sophia E. Economou, “Fast microwave-driven three-qubit gates for cavity-coupled superconducting qubits,” *Phys. Rev. B* **96**, 024504 (2017).
 - [70] Tong Liu, Bao-Qing Guo, Chang-Shui Yu, and Wei-Ning Zhang, “One-step implementation of a hybrid fredkin gate with quantum memories and single superconducting qubit in circuit QED and its applications,” *Opt. Express* **26**, 4498–4511 (2018).
 - [71] M. A. Rol, F. Battistel, F. K. Malinowski, C. C. Bultink, B. M. Tarasinski, R. Vollmer, N. Haider, N. Muthusubramanian, A. Bruno, B. M. Terhal, and L. DiCarlo, “A fast, low-leakage, high-fidelity two-qubit gate for a programmable superconducting quantum computer,” *arXiv e-prints*, arXiv:1903.02492 (2019), arXiv:1903.02492 [quant-ph].
 - [72] Jerry M. Chow, Jay M. Gambetta, A. D. Córcoles, Seth T. Merkel, John A. Smolin, Chad Rigetti, S. Poletto, George A. Keefe, Mary B. Rothwell, J. R. Rozen, Mark B. Ketchen, and M. Steffen, “Universal quantum gate set approaching fault-tolerant thresholds with superconducting qubits,” *Phys. Rev. Lett.* **109**, 060501 (2012).
 - [73] F. D. M. Haldane, “Nonlinear field theory of large-spin Heisenberg antiferromagnets: Semiclassically quantized solitons of the one-dimensional easy-axis Néel state,” *Phys. Rev. Lett.* **50**, 1153–1156 (1983).
 - [74] I Affleck, “Quantum spin chains and the Haldane gap,” *Journal of Physics: Condensed Matter* **1**, 3047 (1989).
 - [75] M. J. Peterer, S. J. Bader, X. Jin, F. Yan, A. Kamal, T. J. Gudmundsen, P. J. Leek, T. P. Orlando, W. D. Oliver, and S. Gustavsson, “Coherence and decay of higher energy levels of a superconducting transmon qubit,” *Phys. Rev. Lett.* **114**, 010501 (2015).
 - [76] E. Kapit, “Hardware-efficient and fully autonomous quantum error correction in superconducting circuits,” *Phys. Rev. Lett.* **116**, 150501 (2016).
 - [77] M. Takita, A. D. Córcoles, E. Magesan, B. Abdo, M. Brink, A. Cross, J. M. Chow, and J. M. Gambetta, “Demonstration of weight-four parity measurements in the surface code architecture,” *Phys. Rev. Lett.* **117**, 210505 (2016).
 - [78] J.R. Johansson, P.D. Nation, and Franco Nori, “Qutip: An open-source python framework for the dynamics of open quantum systems,” *Computer Physics Communications* **183**, 1760 – 1772 (2012).

Supplementary Information

Supplementary Note 1: Derivation of the Hamiltonian for the circuit



Supplementary Figure 1: The superconducting circuit and the corresponding parameters describing the properties of the components. Indicated are also the nodes and the corresponding fluxes.

We are considering the effective circuit in fig. 1 and want to show that the low-energy degrees of freedom of this circuit constitutes three qubits(qutrits) with a Heisenberg XXZ-interaction. We start by writing down the Lagrangian of the system in the node flux picture with the closure branches being the two lower horizontal branches (each splitting into three branches with different circuit elements). The resulting Lagrangian is:

$$\begin{aligned}
 L = & \frac{C_1}{2} (\dot{\phi}_a - \dot{\phi}_c)^2 + \frac{C_1}{2} (\dot{\phi}_b - \dot{\phi}_c)^2 - \frac{1}{2L_1} (\phi_a - \phi_c)^2 - \frac{1}{2\tilde{L}_1} (\phi_b - \phi_c + \Phi_3)^2 \\
 & + \frac{C_2}{2} (\dot{\phi}_a - \dot{\phi}_d)^2 + \frac{C_2}{2} (\dot{\phi}_b - \dot{\phi}_d)^2 - \frac{1}{2L_2} (\phi_a - \phi_d)^2 - \frac{1}{2\tilde{L}_2} (\phi_b - \phi_d + \Phi_6)^2 \\
 & + E_{J1} [\cos(\phi_a - \phi_c + \Phi_1) + \cos(\phi_b - \phi_c + \Phi_2)] \\
 & + E_{J2} [\cos(\phi_a - \phi_d + \Phi_4) + \cos(\phi_b - \phi_d + \Phi_5)] \\
 & + E_{Jq1} \cos(\phi_c) + E_{Jq2} \cos(\phi_a - \phi_b) + E_{Jq3} \cos(\phi_d).
 \end{aligned} \tag{1}$$

Defining $\Phi_{\Sigma 1} = \Phi_1 + \Phi_2$ and assuming $\Phi_1 - \Phi_2 = 0$, we can rewrite the third line using trigonometric identities:

$$2E_{J1} \cos\left(\frac{\phi_a + \phi_b - 2\phi_c + \Phi_{\Sigma 1}}{2}\right) \cos\left(\frac{\phi_a - \phi_b}{2}\right). \quad (2)$$

We will stay in the transmon regime, where the potential terms are much larger than the kinetic terms. This means that we can assume to be close to the potential minimum, approximated to first order by a harmonic oscillator. Thus, we will later rewrite the Hamiltonian in terms of the bosonic step operators related to the harmonic part of the Hamiltonian. We thereafter employ a rotating wave approximation, removing all terms with odd dependence of the node flux variables since these will be energy non-conserving. Specifically these will, after the truncation to the lowest energy levels, represent spontaneous excitation terms. From the Taylor expansion of trigonometric functions, we notice that we can further simplify the expression (2) to the following form using more trigonometric identities:

$$2E_{J1} \cos\left(\frac{\Phi_{\Sigma 1}}{2}\right) \cos\left(\frac{\phi_a + \phi_b - 2\phi_c}{2}\right) \cos\left(\frac{\phi_a - \phi_b}{2}\right). \quad (3)$$

Making the same kind of definition for the fourth term, i.e. $\Phi_{\Sigma 2} = \Phi_4 + \Phi_5$ and assuming $\Phi_4 - \Phi_5 = 0$, we can make the same simplification here. We can also ignore the terms dependent on Φ_3 and Φ_6 as these will again only be irrelevant offset terms or have an odd dependence on the node fluxes. The Lagrangian becomes

$$\begin{aligned} L = & \frac{C_1}{2} (\dot{\phi}_a - \dot{\phi}_c)^2 + \frac{C_1}{2} (\dot{\phi}_b - \dot{\phi}_c)^2 - \frac{1}{2L_1} (\phi_a - \phi_c)^2 - \frac{1}{2\tilde{L}_1} (\phi_b - \phi_c)^2 \\ & + \frac{C_2}{2} (\dot{\phi}_a - \dot{\phi}_d)^2 + \frac{C_2}{2} (\dot{\phi}_b - \dot{\phi}_d)^2 - \frac{1}{2L_2} (\phi_a - \phi_d)^2 - \frac{1}{2\tilde{L}_2} (\phi_b - \phi_d)^2 \\ & + 2E_{J1} \cos\left(\frac{\Phi_{\Sigma 1}}{2}\right) \cos\left(\frac{\phi_a + \phi_b - 2\phi_c}{2}\right) \cos\left(\frac{\phi_a - \phi_b}{2}\right) \\ & + 2E_{J2} \cos\left(\frac{\Phi_{\Sigma 2}}{2}\right) \cos\left(\frac{\phi_a + \phi_b - 2\phi_d}{2}\right) \cos\left(\frac{\phi_a - \phi_b}{2}\right) \\ & + E_{J_{q1}} \cos(\phi_c) + E_{J_{q2}} \cos(\phi_a - \phi_b) + E_{J_{q3}} \cos(\phi_d). \end{aligned}$$

The next step is defining a suitable set of variables. Inspired by the way the ϕ_i 's enter the cosines above, we choose the following:

$$\begin{aligned} \psi_1 &= \phi_a + \phi_b - 2\phi_c \\ \psi_2 &= \phi_a - \phi_b \\ \psi_3 &= \phi_a + \phi_b - 2\phi_d \\ \psi_{CM} &= \phi_a + \phi_b. \end{aligned} \quad (4)$$

In terms of the new variables after expansion of the brackets and collection of terms, the Lagrangian is:

$$\begin{aligned} L = & \frac{C_1}{4} \dot{\psi}_1^2 - \left(\frac{1}{8L_1} + \frac{1}{8\tilde{L}_1}\right) \psi_1^2 + E_{J_{q1}} \cos\left(\frac{\psi_1 - \psi_{CM}}{2}\right) \\ & + \left(\frac{C_1}{4} + \frac{C_2}{4}\right) \dot{\psi}_2^2 - \left(\frac{1}{8L_1} + \frac{1}{8\tilde{L}_1} + \frac{1}{8L_2} + \frac{1}{8\tilde{L}_2}\right) \psi_2^2 + E_{J_{q2}} \cos(\psi_2) \\ & + \frac{C_2}{4} \dot{\psi}_3^2 - \left(\frac{1}{8L_2} + \frac{1}{8\tilde{L}_2}\right) \psi_3^2 + E_{J_{q3}} \cos\left(\frac{\psi_3 - \psi_{CM}}{2}\right) \\ & - \left(\frac{1}{8L_1} - \frac{1}{8\tilde{L}_1}\right) \psi_1 \psi_2 + 2E_{J1} \cos\left(\frac{\Phi_{\Sigma 1}}{2}\right) \cos\left(\frac{\psi_1}{2}\right) \cos\left(\frac{\psi_2}{2}\right) \\ & - \left(\frac{1}{8L_2} - \frac{1}{8\tilde{L}_2}\right) \psi_2 \psi_3 + 2E_{J2} \cos\left(\frac{\Phi_{\Sigma 2}}{2}\right) \cos\left(\frac{\psi_2}{2}\right) \cos\left(\frac{\psi_3}{2}\right). \end{aligned}$$

The conjugate momenta can be found from the usual definition $p_i = \frac{\partial L}{\partial \dot{\psi}_i}$:

$$\begin{aligned} p_1 &= \frac{C_1}{2} \dot{\psi}_1 \\ p_2 &= \left(\frac{C_1}{2} + \frac{C_2}{2} \right) \dot{\psi}_2 \\ p_3 &= \frac{C_2}{2} \dot{\psi}_3 \\ p_{CM} &= 0. \end{aligned} \tag{5}$$

Notice that the conjugate momentum of ψ_{CM} is zero, and thus the variable can be seen as purely a constraint variable without a kinetic term. We will thus ignore ψ_{CM} from now on.

Now performing a Legendre transforming to the Hamiltonian via the relation $H = \sum_i \dot{\psi}_i p_i - L$, we obtain:

$$\begin{aligned} H &= \frac{1}{C_1} p_1^2 + \left(\frac{1}{8L_1} + \frac{1}{8\tilde{L}_1} \right) \psi_1^2 - E_{J_{q1}} \cos \left(\frac{\psi_1}{2} \right) \\ &+ \frac{1}{C_1 + C_2} p_2^2 + \left(\frac{1}{8L_1} + \frac{1}{8\tilde{L}_1} + \frac{1}{8L_2} + \frac{1}{8\tilde{L}_2} \right) \psi_2^2 - E_{J_{q2}} \cos(\psi_2) \\ &+ \frac{1}{C_2} p_3^2 + \left(\frac{1}{8L_2} + \frac{1}{8\tilde{L}_2} \right) \psi_3^2 - E_{J_{q3}} \cos \left(\frac{\psi_3}{2} \right) \\ &+ \left(\frac{1}{8L_1} - \frac{1}{8\tilde{L}_1} \right) \psi_1 \psi_2 - 2E_{J1} \cos \left(\frac{\Phi_{\Sigma 1}}{2} \right) \cos \left(\frac{\psi_1}{2} \right) \cos \left(\frac{\psi_2}{2} \right) \\ &+ \left(\frac{1}{8L_2} - \frac{1}{8\tilde{L}_2} \right) \psi_2 \psi_3 - 2E_{J2} \cos \left(\frac{\Phi_{\Sigma 2}}{2} \right) \cos \left(\frac{\psi_2}{2} \right) \cos \left(\frac{\psi_3}{2} \right). \end{aligned}$$

The cosines are now expanded to fourth order in the flux variables:

$$\begin{aligned} \cos(x) &\simeq 1 - \frac{1}{2}x^2 + \frac{1}{24}x^4 \\ \cos\left(\frac{x}{2}\right) &\simeq 1 - \frac{1}{8}x^2 + \frac{1}{384}x^4 \\ \cos\left(\frac{x_1}{2}\right) \cos\left(\frac{x_2}{2}\right) &\simeq 1 - \frac{1}{8}x_1^2 + \frac{1}{384}x_1^4 - \frac{1}{8}x_2^2 + \frac{1}{384}x_2^4 + \frac{1}{64}x_1^2 x_2^2. \end{aligned} \tag{6}$$

This approximation neglects six-order terms and higher. Using first-order perturbation theory on the sixth-order term from $\cos(\psi_2)$ above, we get a correction to the final ground state energy of the corresponding qubit of $E^{(1)}/(2\pi) \simeq 31$ kHz. This can safely be ignored compared to the usual transmon energies in the order of 10 GHz. Also, since we make sure to stay in the transmon limit with the potential terms much higher than the kinetic terms, we will always stay near very small values of the transmon phase drops, which is the physical interpretation of the flux variables, ψ_i . This makes, up to irrelevant constant terms,

$$\begin{aligned} H &= \frac{1}{C_1} p_1^2 + \alpha_1 \psi_1^2 - \beta_1 \psi_1^4 \\ &+ \frac{1}{C_1 + C_2} p_2^2 + \alpha_2 \psi_2^2 - \beta_2 \psi_2^4 \\ &+ \frac{1}{C_2} p_3^2 + \alpha_3 \psi_3^2 - \beta_3 \psi_3^4 \\ &+ \left(\frac{1}{8L_1} - \frac{1}{8\tilde{L}_1} \right) \psi_1 \psi_2 - \frac{E_{J1}}{32} \cos \left(\frac{\Phi_{\Sigma 1}}{2} \right) \psi_1^2 \psi_2^2 \\ &+ \left(\frac{1}{8L_2} - \frac{1}{8\tilde{L}_2} \right) \psi_2 \psi_3 - \frac{E_{J2}}{32} \cos \left(\frac{\Phi_{\Sigma 2}}{2} \right) \psi_2^2 \psi_3^2, \end{aligned}$$

where

$$\begin{aligned}
\alpha_1 &= \frac{1}{8L_1} + \frac{1}{8\tilde{L}_1} + \frac{E_{J_{q1}}}{8} + \frac{E_{J1}}{4} \cos\left(\frac{\Phi_{\Sigma1}}{2}\right) \\
\beta_1 &= \frac{E_{J_{q1}}}{384} + \frac{E_{J1}}{192} \cos\left(\frac{\Phi_{\Sigma1}}{2}\right) \\
\alpha_2 &= \frac{1}{8L_1} + \frac{1}{8\tilde{L}_1} + \frac{1}{8L_2} + \frac{1}{8\tilde{L}_2} + \frac{E_{J_{q2}}}{2} + \frac{E_{J1}}{4} \cos\left(\frac{\Phi_{\Sigma1}}{2}\right) + \frac{E_{J2}}{4} \cos\left(\frac{\Phi_{\Sigma2}}{2}\right) \\
\beta_2 &= \frac{E_{J_{q2}}}{24} + \frac{E_{J1}}{192} \cos\left(\frac{\Phi_{\Sigma1}}{2}\right) + \frac{E_{J2}}{192} \cos\left(\frac{\Phi_{\Sigma2}}{2}\right) \\
\alpha_3 &= \frac{1}{8L_2} + \frac{1}{8\tilde{L}_2} + \frac{E_{J_{q3}}}{8} + \frac{E_{J2}}{4} \cos\left(\frac{\Phi_{\Sigma2}}{2}\right) \\
\beta_3 &= \frac{E_{J_{q3}}}{384} + \frac{E_{J2}}{192} \cos\left(\frac{\Phi_{\Sigma2}}{2}\right).
\end{aligned} \tag{7}$$

Taking the anharmonicity (fourth-order terms) as a perturbation, we now choose the bosonic raising and lowering operators related to the harmonic parts of the Hamiltonian (the p^2 and ψ^2 -terms) above as usual (This perturbation is essential for the later truncation, since the resulting anharmonicity of the energy spacing between the levels allows us to only consider the lowest states):

$$\begin{aligned}
\psi_1 &= \frac{1}{(4\alpha_1 C_1)^{\frac{1}{4}}} (b_1^\dagger + b_1) \\
\psi_2 &= \frac{1}{(4\alpha_2 (C_1 + C_2))^{\frac{1}{4}}} (b_2^\dagger + b_2) \\
\psi_3 &= \frac{1}{(4\alpha_3 C_2)^{\frac{1}{4}}} (b_3^\dagger + b_3).
\end{aligned} \tag{8}$$

We end up with the rewritten Hamiltonian

$$\begin{aligned}
H &= \sqrt{\frac{4\alpha_1}{C_1}} \left(b_1^\dagger b_1 + \frac{1}{2} \right) - \frac{\beta_1}{4\alpha_1 C_1} (b_1^\dagger + b_1)^4 \\
&+ \sqrt{\frac{4\alpha_2}{C_1 + C_2}} \left(b_2^\dagger b_2 + \frac{1}{2} \right) - \frac{\beta_2}{4\alpha_2 (C_1 + C_2)} (b_2^\dagger + b_2)^4 \\
&+ \sqrt{\frac{4\alpha_3}{C_2}} \left(b_3^\dagger b_3 + \frac{1}{2} \right) - \frac{\beta_3}{4\alpha_3 C_2} (b_3^\dagger + b_3)^4 \\
&+ \left(\frac{1}{8L_1} - \frac{1}{8\tilde{L}_1} \right) \frac{1}{2(\alpha_1 \alpha_2 C_1 (C_1 + C_2))^{\frac{1}{4}}} (b_1^\dagger + b_1) (b_2^\dagger + b_2) \\
&- \frac{E_{J1}}{128} \cos\left(\frac{\Phi_{\Sigma1}}{2}\right) \frac{1}{\sqrt{\alpha_1 \alpha_2 C_1 (C_1 + C_2)}} (b_1^\dagger + b_1)^2 (b_2^\dagger + b_2)^2 \\
&+ \left(\frac{1}{8L_2} - \frac{1}{8\tilde{L}_2} \right) \frac{1}{2(\alpha_2 \alpha_3 C_2 (C_1 + C_2))^{\frac{1}{4}}} (b_2^\dagger + b_2) (b_3^\dagger + b_3) \\
&- \frac{E_{J2}}{128} \cos\left(\frac{\Phi_{\Sigma2}}{2}\right) \frac{1}{\sqrt{\alpha_2 \alpha_3 C_2 (C_1 + C_2)}} (b_2^\dagger + b_2)^2 (b_3^\dagger + b_3)^2.
\end{aligned} \tag{9}$$

We could now in principle map this to a spin model by using the anharmonicity to truncate to the lowest two/three energy eigenstates (e.g. $b_i^\dagger + b_i \mapsto \sigma_i^x$ for a qubit) and after using the rotating wave approximation end up with a Hamiltonian with the desired form. This would have the drawback of being static, i.e. once the circuit is built to certain specifications the experimental parameters are fixed and the energy levels and coupling strengths can not be adjusted significantly afterwards. We will introduce a dynamical tuning by adding an external driving field, effectively mixing the first and second excited state of the middle (ψ_2) degree of freedom and thereby changing the energy levels and coupling strengths.

Adding an effective external energy level tuning

We now imagine control lines connecting to the nodes a and b as in the main text. These can then be used to drive the middle degree of freedom ψ_2 using external fields. Specifically, we let the control line 5 connect to the node with flux ϕ_a

in Supplementary Fig. 1 through the capacitance C_{ext} and drive an external field ϕ_{ext} . Similarly, we apply an external field $\phi_{-\text{ext}}$ through control line 6 connected to the node flux ϕ_b through the same capacitance C_{ext} . The following extra term will appear in the Lagrangian:

$$L_{\text{ext}} = \frac{C_{\text{ext}}}{2} (\dot{\phi}_a - \dot{\phi}_{\text{ext}})^2 + \frac{C_{\text{ext}}}{2} (\dot{\phi}_b - \dot{\phi}_{-\text{ext}})^2. \quad (10)$$

This can be rewritten to

$$L_{\text{ext}} = \frac{C_{\text{ext}}}{4} \left[(\dot{\phi}_a + \dot{\phi}_b - \dot{\phi}_{-\text{ext}} - \dot{\phi}_{\text{ext}})^2 + (\dot{\phi}_a - \dot{\phi}_b + \dot{\phi}_{-\text{ext}} - \dot{\phi}_{\text{ext}})^2 \right].$$

Assuming $\phi_{\text{ext}} = -\phi_{-\text{ext}} = A_{\text{ext}} \sin(\omega_{\text{ext}} t)$ and transforming to the ψ -coordinates, this reduces to

$$\begin{aligned} L_{\text{ext}} &= \frac{C_{\text{ext}}}{4} \left[\dot{\psi}_{CM}^2 + (\dot{\psi}_2 - 2A_{\text{ext}}\omega_{\text{ext}} \cos(\omega_{\text{ext}} t))^2 \right] \\ &= \frac{C_{\text{ext}}}{4} \dot{\psi}_{CM}^2 + \frac{C_{\text{ext}}}{4} \dot{\psi}_2^2 + C_{\text{ext}} A_{\text{ext}}^2 \omega_{\text{ext}}^2 \cos^2(\omega_{\text{ext}} t) - C_{\text{ext}} \dot{\psi}_2 A_{\text{ext}} \omega_{\text{ext}} \cos(\omega_{\text{ext}} t). \end{aligned} \quad (11)$$

The first term here is an apparently problematic kinetic term for what has so far been a constraint variable. This can, though, be constructed to have a spacing between the energy levels that is very far from the spacing of the other degrees of freedom and ψ_{CM} can thus be ignored in spite of this term. The second term is another kinetic term for the ψ_2 -variable, the third term is an offset term, and the fourth and last term is an interaction term between ψ_2 and the external field. It is this last term that will be useful for driving transitions between, and hence coupling of, the first and second excited levels of ψ_2 . This will allow us to tune the position of the two levels through non-crossing depending on how much we mix the states.

Including the above addition, the Lagrangian related purely to the ψ_2 -degree of freedom is the following:

$$L_2 = \frac{C_1 + C_2 + C_{\text{ext}}}{4} \dot{\psi}_2^2 - \left(\frac{1}{8L_1} + \frac{1}{8\tilde{L}_1} + \frac{1}{8L_2} + \frac{1}{8\tilde{L}_2} \right) \psi_2^2 + E_{J_{q2}} \cos(\psi_2) - C_{\text{ext}} A_{\text{ext}} \omega_{\text{ext}} \cos(\omega_{\text{ext}} t) \dot{\psi}_2,$$

with all other terms being either purely related to ψ_1 or ψ_3 or interaction terms. The corresponding conjugated momentum is also altered slightly:

$$p_2 = \frac{C_1 + C_2 + C_{\text{ext}}}{2} \dot{\psi}_2 - C_{\text{ext}} A_{\text{ext}} \omega_{\text{ext}} \cos(\omega_{\text{ext}} t), \quad (12)$$

thus

$$\dot{\psi}_2 = \frac{2}{C_1 + C_2 + C_{\text{ext}}} (p_2 + C_{\text{ext}} A_{\text{ext}} \omega_{\text{ext}} \cos(\omega_{\text{ext}} t)). \quad (13)$$

The related Hamiltonian is therefore, ignoring any offset terms:

$$\begin{aligned} H_2 &= \frac{p_2^2}{C_1 + C_2 + C_{\text{ext}}} + \frac{2C_{\text{ext}} A_{\text{ext}} \omega_{\text{ext}} \cos(\omega_{\text{ext}} t)}{C_1 + C_2 + C_{\text{ext}}} p_2 \\ &\quad + \left(\frac{1}{8L_1} + \frac{1}{8\tilde{L}_1} + \frac{1}{8L_2} + \frac{1}{8\tilde{L}_2} \right) \psi_2^2 - E_{J_{q2}} \cos(\psi_2). \end{aligned}$$

Performing the same expansions as before addition of the extra capacitances and external fields gives a few extra ψ_2 -terms from the interaction terms. Focusing on only the resulting terms containing only ψ_2 or p_2 , we get:

$$H_2 = \frac{1}{C_1 + C_2 + C_{\text{ext}}} p_2^2 + \alpha_2 \psi_2^2 - \beta_2 \psi_2^4 + \frac{2C_{\text{ext}} A_{\text{ext}} \omega_{\text{ext}} \cos(\omega_{\text{ext}} t)}{C_1 + C_2 + C_{\text{ext}}} p_2, \quad (14)$$

where α_2 and β_2 are defined in (7). We once again introduce the bosonic step-operators related to the harmonic part of H_2 :

$$\begin{aligned} \psi_2 &= \frac{1}{(4\alpha_2(C_1 + C_2 + C_{\text{ext}}))^{\frac{1}{4}}} (b_2^\dagger + b_2) \\ p_2 &= i \frac{(4\alpha_2(C_1 + C_2 + C_{\text{ext}}))^{\frac{1}{4}}}{2} (b_2^\dagger - b_2), \end{aligned} \quad (15)$$

which makes

$$H_2 = T_1 b_2^\dagger b_2 - T_2 (b_2^\dagger + b_2)^4 + iT_{\text{ext}} \cos(\omega_{\text{ext}} t) (b_2^\dagger - b_2), \quad (16)$$

where

$$\begin{aligned}
T_1 &= \sqrt{\frac{4\alpha_2}{C_1 + C_2 + C_{\text{ext}}}} \\
T_2 &= \frac{\beta_2}{4\alpha_2(C_1 + C_2 + C_{\text{ext}})} \\
T_{\text{ext}} &= C_{\text{ext}} A_{\text{ext}} \omega_{\text{ext}} \frac{(4\alpha_2(C_1 + C_2 + C_{\text{ext}}))^{\frac{1}{4}}}{C_1 + C_2 + C_{\text{ext}}}.
\end{aligned} \tag{17}$$

We wish to diagonalize this Hamiltonian to investigate the effect of T_{ext} on the spectrum.

Truncating the middle degree of freedom

We will now investigate the dynamical tuning of the spectrum by first truncating the “internal” Hamiltonian for the ψ_2 degree of freedom, corresponding to setting $A_{\text{ext}} = 0$, to the three lowest degrees of freedom, i.e. find the qutrit eigenstates. We will then add the external field and transform to a frame rotating with the external field, wherein we can see the effective mixing of the qutrit eigenstates. Lastly, we shift basis and use these driven states in the rotating frame as our qutrit eigenstates.

We start by diagonalizing the internal Hamiltonian of the middle degree of freedom “ $H_{2,0}$ ”, i.e. the first two terms in (16): In the basis of the three lowest simple harmonic oscillator states, which is chosen since we wish to end up with a qutrit in the end, we represent (up to irrelevant offset terms proportional to the identity)

$$b_2^\dagger \sim \begin{pmatrix} 0 & 0 & 0 \\ 1 & 0 & 0 \\ 0 & \sqrt{2} & 0 \end{pmatrix}, \quad b_2 \sim \begin{pmatrix} 0 & 1 & 0 \\ 0 & 0 & \sqrt{2} \\ 0 & 0 & 0 \end{pmatrix}. \tag{18}$$

This truncation is also done for all terms in (16), after using the canonical commutation relation $[b, b^\dagger] = 1$ to transform to normal ordering form:

$$b_2^\dagger b_2 \sim \begin{pmatrix} 0 & 0 & 0 \\ 0 & 1 & 0 \\ 0 & 0 & 2 \end{pmatrix}, \quad (b_2^\dagger + b_2)^4 \sim \begin{pmatrix} 0 & 0 & 6\sqrt{2} \\ 0 & 12 & 0 \\ 6\sqrt{2} & 0 & 36 \end{pmatrix},$$

and

$$b_2^\dagger - b_2 \sim \begin{pmatrix} 0 & -1 & 0 \\ 1 & 0 & -\sqrt{2} \\ 0 & \sqrt{2} & 0 \end{pmatrix}$$

Inserting this in the first two terms in equation (16), we get the Hamiltonian

$$H_{2,0} \sim \begin{pmatrix} 0 & 0 & -6\sqrt{2}T_2 \\ 0 & T_1 - 12T_2 & 0 \\ -6\sqrt{2}T_2 & 0 & 2T_1 - 36T_2 \end{pmatrix},$$

which has the eigenenergies:

$$\begin{aligned}
E_0 &= T_1 - 18T_2 - \sqrt{(T_1 - 18T_2)^2 + 72T_2^2} \\
E_1 &= T_1 - 12T_2 \\
E_2 &= T_1 - 18T_2 + \sqrt{(T_1 - 18T_2)^2 + 72T_2^2}
\end{aligned} \tag{19}$$

with the corresponding eigenstates:

$$\begin{aligned}
|\tilde{0}\rangle &= \frac{1}{\sqrt{72T_2^2 + E_0^2}} \begin{pmatrix} 6\sqrt{2}T_2 \\ 0 \\ -E_0 \end{pmatrix} \\
|\tilde{1}\rangle &= \begin{pmatrix} 0 \\ 1 \\ 0 \end{pmatrix} \\
|\tilde{2}\rangle &= \frac{1}{\sqrt{72T_2^2 + E_2^2}} \begin{pmatrix} -6\sqrt{2}T_2 \\ 0 \\ E_2 \end{pmatrix}.
\end{aligned} \tag{20}$$

Now turning on the full external field, the full Hamiltonian H_2 can be expressed as

$$H_2 = E_0 |\tilde{0}\rangle\langle\tilde{0}| + E_1 |\tilde{1}\rangle\langle\tilde{1}| + E_2 |\tilde{2}\rangle\langle\tilde{2}| + \frac{T_{\text{ext}}}{2} (e^{i\omega_{\text{ext}}t} + e^{-i\omega_{\text{ext}}t}) \begin{pmatrix} 0 & -i & 0 \\ i & 0 & -\sqrt{2}i \\ 0 & \sqrt{2}i & 0 \end{pmatrix}, \quad (21)$$

where the first three terms are the bare qutrit eigenstates and the last matrix is written in the old basis ($|0\rangle, |1\rangle, |2\rangle$). The outer degrees of freedom (1, 3) is truncated to the lowest two degrees levels (i.e. an effective qubit) as is standard, where $|\uparrow\rangle$ and $|\downarrow\rangle$ will denote the excited and ground state, respectively.

We now switch to a rotating frame corresponding to the external field, which means performing a unitary transformation with the operator:

$$U_{\text{ext}} = U_{\text{ext},1} U_{\text{ext},2} U_{\text{ext},3}, \quad (22)$$

where

$$U_{\text{ext},\alpha} = e^{i\omega_{\text{ext}}t/2} |\downarrow\rangle\langle\downarrow| + e^{-i\omega_{\text{ext}}t/2} |\uparrow\rangle\langle\uparrow|, \quad (23)$$

for $\alpha = 1, 3$, and

$$U_{\text{ext},2}(t) = e^{i3\omega_{\text{ext}}t/2} |\tilde{0}\rangle\langle\tilde{0}| + e^{i\omega_{\text{ext}}t/2} |\tilde{1}\rangle\langle\tilde{1}| + e^{-i\omega_{\text{ext}}t/2} |\tilde{2}\rangle\langle\tilde{2}|. \quad (24)$$

We are trying to obtain a mixing of the first and second energy levels and therefore assume that we can tune ω_{ext} so that it is close to $E_2 - E_1$ and far from $E_1 - E_0$ and $E_2 - E_0$, effectively enabling us to perform the two-level approximation. A transformation of the Hamiltonian can now be performed according to the standard transformation rule

$$H \rightarrow H^R = U_{\text{ext}}^\dagger H U_{\text{ext}} + i \frac{dU_{\text{ext}}^\dagger}{dt} U_{\text{ext}}. \quad (25)$$

Since our Hamiltonian is quite big, we take this one part at a time. Starting with the terms purely related to the ψ_2 degree of freedom, it is a good idea to look at the matrix elements from the last factor in (21) when performing this transformation:

$$\langle\tilde{1}| \left(|1\rangle\langle 0| - \sqrt{2} |1\rangle\langle 2| \right) |\tilde{2}\rangle = - \frac{\sqrt{2}(6T_2 + E_2)}{\sqrt{(6\sqrt{2}T_2)^2 + E_2^2}} \quad (26)$$

$$\langle\tilde{2}| \left(-|0\rangle\langle 1| + \sqrt{2} |2\rangle\langle 1| \right) |\tilde{1}\rangle = \frac{\sqrt{2}(6T_2 + E_2)}{\sqrt{(6\sqrt{2}T_2)^2 + E_2^2}}, \quad (27)$$

where the rest are either irrelevant or zero. So, we get in the rotating frame

$$\begin{aligned} H_2 &= E_0 |\tilde{0}\rangle\langle\tilde{0}| + E_1 |\tilde{1}\rangle\langle\tilde{1}| + E_2 |\tilde{2}\rangle\langle\tilde{2}| \\ &+ i \frac{T_{\text{ext}}}{2} \frac{\sqrt{2}(6T_2 + E_2)}{\sqrt{(6\sqrt{2}T_2)^2 + E_2^2}} (e^{i\omega_{\text{ext}}t} + e^{-i\omega_{\text{ext}}t}) (-|\tilde{1}\rangle\langle\tilde{2}| e^{-i\omega_{\text{ext}}t} + |\tilde{2}\rangle\langle\tilde{1}| e^{i\omega_{\text{ext}}t}) \\ &+ \frac{3\omega_{\text{ext}}}{2} |\tilde{0}\rangle\langle\tilde{0}| + \frac{\omega_{\text{ext}}}{2} |\tilde{1}\rangle\langle\tilde{1}| - \frac{\omega_{\text{ext}}}{2} |\tilde{2}\rangle\langle\tilde{2}| \\ &= \left(E_0 + \frac{3\omega_{\text{ext}}}{2} \right) |\tilde{0}\rangle\langle\tilde{0}| + \left(E_1 + \frac{\omega_{\text{ext}}}{2} \right) |\tilde{1}\rangle\langle\tilde{1}| + \left(E_2 - \frac{\omega_{\text{ext}}}{2} \right) |\tilde{2}\rangle\langle\tilde{2}| \\ &\quad - i\Delta \left[|\tilde{1}\rangle\langle\tilde{2}| (1 + e^{-2i\omega_{\text{ext}}t}) - |\tilde{2}\rangle\langle\tilde{1}| (1 + e^{2i\omega_{\text{ext}}t}) \right] \\ &\simeq \left(E_0 + \frac{3\omega_{\text{ext}}}{2} \right) |\tilde{0}\rangle\langle\tilde{0}| + \left(E_1 + \frac{\omega_{\text{ext}}}{2} \right) |\tilde{1}\rangle\langle\tilde{1}| + \left(E_2 - \frac{\omega_{\text{ext}}}{2} \right) |\tilde{2}\rangle\langle\tilde{2}| + i\Delta \left(|\tilde{2}\rangle\langle\tilde{1}| - |\tilde{1}\rangle\langle\tilde{2}| \right), \end{aligned} \quad (28)$$

where we in the last equation has used the rotating wave approximation to remove the fast oscillating terms $\exp(\pm 2i\omega_{\text{ext}}t)$, and we have defined

$$\Delta = \frac{T_{\text{ext}}}{2} \frac{\sqrt{2}(E_2 + 6T_2)}{\sqrt{(6\sqrt{2}T_2)^2 + E_2^2}}. \quad (29)$$

Writing this in terms of the detuning from resonance

$$\delta = E_2 - E_1 - \omega_{\text{ext}}, \quad (30)$$

we can rewrite the expression above as

$$H_2^R = \left(\frac{E_1 + E_2}{2} + \xi - \frac{3\delta}{2} \right) |\tilde{0}\rangle\langle\tilde{0}| + \left(\frac{E_1 + E_2}{2} - \frac{\delta}{2} \right) |\tilde{1}\rangle\langle\tilde{1}| + \left(\frac{E_1 + E_2}{2} + \frac{\delta}{2} \right) |\tilde{2}\rangle\langle\tilde{2}| + i\Delta \left(|\tilde{2}\rangle\langle\tilde{1}| - |\tilde{1}\rangle\langle\tilde{2}| \right) \quad (31)$$

or, representing this in the matrix representation in the tilde states as basis states:

$$H_2^R \sim \begin{pmatrix} \xi - \frac{3\delta}{2} & 0 & 0 \\ 0 & -\frac{\delta}{2} & -i\Delta \\ 0 & i\Delta & \frac{\delta}{2} \end{pmatrix} + \frac{E_1 + E_2}{2} \mathbb{I}_3,$$

where \mathbb{I}_3 is the 3×3 identity matrix of the qutrit, which can be safely ignored, and $\xi = E_2 - E_1 - (E_1 - E_0) < 0$ is the absolute anharmonicity between the first and second level in the qutrit. This can be diagonalized to find the energy spectrum

$$\begin{aligned} E'_0 &= \xi - \frac{3\delta}{2} \\ E'_1 &= -\gamma \\ E'_2 &= +\gamma, \end{aligned} \quad (32)$$

where

$$\gamma = \frac{1}{2} \sqrt{\delta^2 + 4\Delta^2}. \quad (33)$$

The (normalized) eigenstates of this Hamiltonian, expressed in the basis $\{|\tilde{0}\rangle, |\tilde{1}\rangle, |\tilde{2}\rangle\}$, are

$$\begin{aligned} |0'\rangle &\sim \begin{pmatrix} 1 \\ 0 \\ 0 \end{pmatrix} \\ |1'\rangle &\sim \frac{1}{\sqrt{\Delta^2 + \left(\frac{\delta}{2} - \gamma\right)^2}} \begin{pmatrix} 0 \\ i\Delta \\ -\frac{\delta}{2} + \gamma \end{pmatrix} \\ |2'\rangle &\sim \frac{1}{\sqrt{\Delta^2 + \left(\frac{\delta}{2} + \gamma\right)^2}} \begin{pmatrix} 0 \\ -i\Delta \\ \frac{\delta}{2} + \gamma \end{pmatrix}. \end{aligned} \quad (34)$$

In the limit $\Delta \rightarrow 0$, these reduce to the bare energy states $|i'\rangle \rightarrow |\tilde{i}\rangle$ for $i = 0, 1, 2$ when $\delta > 0$ meaning the driving frequency is below the undriven energy difference between the upper qutrit states. The Hamiltonian for the ψ_2 degree of freedom reduces to

$$H_2^R = E'_0 |0'\rangle\langle 0'| + E'_1 |1'\rangle\langle 1'| + E'_2 |2'\rangle\langle 2'| = E'_0 \mathbb{I}_2 + (E'_1 - E'_0) |1'\rangle\langle 1'| + (E'_2 - E'_0) |2'\rangle\langle 2'|, \quad (35)$$

where the diagonal term will again be throw away from this point onwards. In conclusion, we see that by tuning A_{ext} and/or ω_{ext} , we can change E'_1 and E'_2 , i.e. the contribution of the part of the Hamiltonian purely related to ψ_2 to the energy of the two highest qutrit states.

Next, we perform the transformation to the rotating picture to the parts of the Hamiltonian purely related to the outer fluxes $j = 1, 3$. We choose the qubit spin-up state as the excited state, e.g. we associate $b_j^\dagger b_j \mapsto \frac{1}{2} + \frac{1}{2} \sigma_j^z$. Thus

$$H_j \rightarrow H_j^R = U_{\text{ext},j}^\dagger \left[\sqrt{\frac{4\alpha_j}{C_j}} \left(b_j^\dagger b_j + \frac{1}{2} \right) - \frac{\beta_j}{4\alpha_j C_j} (b_j^\dagger + b_j)^4 \right] U_{\text{ext},\alpha} \quad (36)$$

$$= \frac{1}{2} \left(\sqrt{\frac{4\alpha_j}{C_j}} - \frac{3\beta_j}{\alpha_j C_j} \right) \sigma_j^z + \frac{\omega_{\text{ext}}}{2} |\downarrow\rangle\langle\downarrow| - \frac{\omega_{\text{ext}}}{2} |\uparrow\rangle\langle\uparrow| \quad (37)$$

$$= \frac{1}{2} \left(\sqrt{\frac{4\alpha_j}{C_j}} - \frac{3\beta_j}{\alpha_j C_j} - \omega_{\text{ext}} \right) \sigma_j^z, \quad (38)$$

where we have made the usual truncation to a qubit.

We have yet to do the transformation to the rotating picture for the interaction terms. The factors involved are $(b_j^\dagger + b_j)$, which normally for a qubit maps to σ_j^x before moving to the interaction picture, and $(b_j^\dagger + b_j)^2$, which maps to $2 + \sigma_j^z$ for a qubit. We start by looking at the factor (for $j = 1, 3$):

$$(b_2^\dagger + b_2)(b_j^\dagger + b_j) \rightarrow U_{\text{ext},2}^\dagger (b_2^\dagger + b_2) U_{\text{ext},2} U_{\text{ext},j}^\dagger (b_j^\dagger + b_j) U_{\text{ext},j}.$$

The first factor is:

$$U_{\text{ext},2}^\dagger (b_2^\dagger + b_2) U_{\text{ext},2} = k_0 (e^{-i\omega_{\text{ext}} t} |\tilde{0}\rangle\langle\tilde{1}| + e^{i\omega_{\text{ext}} t} |\tilde{1}\rangle\langle\tilde{0}|) + k_2 (e^{-i\omega_{\text{ext}} t} |\tilde{1}\rangle\langle\tilde{2}| + e^{i\omega_{\text{ext}} t} |\tilde{2}\rangle\langle\tilde{1}|), \quad (39)$$

where

$$k_i = (-1)^{\frac{i}{2}} \frac{\sqrt{2}(6T_2 - E_i)}{\sqrt{(6\sqrt{2}T_2)^2 + E_i^2}} \quad (40)$$

for $i = 0, 2$. The second factor contributes with:

$$U_{\text{ext},j}^\dagger (b_j^\dagger + b_j) U_{\text{ext},j} = e^{-i\omega_{\text{ext}} t} |\downarrow\rangle\langle\uparrow| + e^{i\omega_{\text{ext}} t} |\uparrow\rangle\langle\downarrow|. \quad (41)$$

So:

$$(b_2^\dagger + b_2)(b_j^\dagger + b_j) \rightarrow k_0 (\sigma_j^+ |\tilde{0}\rangle\langle\tilde{1}| + \sigma_j^- |\tilde{1}\rangle\langle\tilde{0}| + e^{-i2\omega_{\text{ext}} t} \sigma_j^- |\tilde{0}\rangle\langle\tilde{1}| + e^{i2\omega_{\text{ext}} t} \sigma_j^+ |\tilde{1}\rangle\langle\tilde{0}|) \quad (42)$$

$$+ k_2 (\sigma_j^+ |\tilde{1}\rangle\langle\tilde{2}| + \sigma_j^- |\tilde{2}\rangle\langle\tilde{1}| + e^{-i2\omega_{\text{ext}} t} \sigma_j^- |\tilde{1}\rangle\langle\tilde{2}| + e^{i2\omega_{\text{ext}} t} \sigma_j^+ |\tilde{2}\rangle\langle\tilde{1}|) \quad (43)$$

$$\simeq k_0 (\sigma_j^+ |\tilde{0}\rangle\langle\tilde{1}| + \sigma_j^- |\tilde{1}\rangle\langle\tilde{0}|) + k_2 (\sigma_j^+ |\tilde{1}\rangle\langle\tilde{2}| + \sigma_j^- |\tilde{2}\rangle\langle\tilde{1}|), \quad (44)$$

where we in the last equality have used the rotating wave approximation to remove the fast oscillating terms. Since we want to look at the primed mixed states as the new tunable qutrit, we transform this to the primed basis:

$$(b_2^\dagger + b_2)(b_j^\dagger + b_j) \rightarrow k_0 \sigma_j^+ \langle\tilde{1}|1'\rangle |0'\rangle\langle 1'| + k_0 \sigma_j^- \langle 1'|\tilde{1}\rangle |1'\rangle\langle 0'| \quad (45)$$

$$+ k_2 (\sigma_j^+ \langle 1'|\tilde{1}\rangle \langle\tilde{2}|1'\rangle + \sigma_j^- \langle 1'|\tilde{2}\rangle \langle\tilde{1}|1'\rangle) |1'\rangle\langle 1'| \quad (46)$$

$$+ k_2 (\sigma_j^+ \langle 1'|\tilde{1}\rangle \langle\tilde{2}|2'\rangle + \sigma_j^- \langle 1'|\tilde{2}\rangle \langle\tilde{1}|2'\rangle) |1'\rangle\langle 2'| \quad (47)$$

$$+ k_2 (\sigma_j^+ \langle 2'|\tilde{1}\rangle \langle\tilde{2}|1'\rangle + \sigma_j^- \langle 2'|\tilde{2}\rangle \langle\tilde{1}|1'\rangle) |2'\rangle\langle 1'| \quad (48)$$

$$+ k_2 (\sigma_j^+ \langle 2'|\tilde{1}\rangle \langle\tilde{2}|2'\rangle + \sigma_j^- \langle 2'|\tilde{2}\rangle \langle\tilde{1}|2'\rangle) |2'\rangle\langle 2'| \quad (49)$$

$$+ k_0 \sigma_j^+ \langle\tilde{1}|2'\rangle |0'\rangle\langle 2'| + k_0 \sigma_j^- \langle 2'|\tilde{1}\rangle |2'\rangle\langle 0'|. \quad (50)$$

Some of these terms look troubling, but luckily, all terms proportional with an off-diagonal overlap between the primed and tilde states will be much smaller than the diagonal ones and can be ignored. Also, all these terms are general energy non-conserving and thus could also be eliminated using a rotating wave approximation in the interaction picture. We note that the imaginary factor from the matrix elements can be eliminated by defining $|1'\rangle \mapsto |1'\rangle_{\text{new}} = -i|1'\rangle_{\text{old}}$. We thus end with:

$$(b_2^\dagger + b_2)(b_j^\dagger + b_j) \xrightarrow{\text{R}} \frac{k_0 \Delta}{\sqrt{\Delta^2 + (\frac{\delta}{2} - \gamma)^2}} (\sigma_j^+ |0'\rangle\langle 1'| + \sigma_j^- |1'\rangle\langle 0'|) \quad (51)$$

$$+ \frac{k_2 (\frac{\delta}{2} + \gamma)}{2\gamma} (\sigma_j^+ |1'\rangle\langle 2'| + \sigma_j^- |2'\rangle\langle 1'|), \quad (52)$$

where the “R” denotes the transformation to the rotating frame. We note that the couplings $|0'\rangle \leftrightarrow |1'\rangle$ and $|1'\rangle \leftrightarrow |2'\rangle$ are not equal. In fact, for small Δ , the latter is a factor of $\sqrt{2}$ bigger, originating from the definition of the bosonic step operators.

We can now look at the transformation of the last kind of interaction term:

$$(b_2^\dagger + b_2)^2 (b_j^\dagger + b_j)^2 \rightarrow U_{\text{ext},2}^\dagger (b_2^\dagger + b_2)^2 U_{\text{ext},2} U_{\text{ext},j}^\dagger (b_j^\dagger + b_j)^2 U_{\text{ext},j}. \quad (53)$$

For the second factor, the transformation is equal to the identity for the standard qubit basis, i.e.

$$U_{\text{ext},j}^\dagger (b_j^\dagger + b_j)^2 U_{\text{ext},j} \mapsto 2 + \sigma_j^z. \quad (54)$$

Performing the transformation for the first factor, we get:

$$\begin{aligned} U_{\text{ext},2}^\dagger (b_2^\dagger + b_2)^2 U_{\text{ext},2} &= C_{00} |\tilde{0}\rangle\langle\tilde{0}| + 3 |\tilde{1}\rangle\langle\tilde{1}| + C_{22} |\tilde{2}\rangle\langle\tilde{2}| \\ &\quad + C_{02} \left(e^{-i2\omega_{\text{ext}}t} |\tilde{0}\rangle\langle\tilde{2}| + e^{i2\omega_{\text{ext}}t} |\tilde{2}\rangle\langle\tilde{0}| \right). \end{aligned} \quad (55)$$

Again, the last two terms are fast-rotating and can be removed. We have defined:

$$\begin{aligned} C_{00} &= 1 - \frac{4E_0(6T_2 - E_0)}{(6\sqrt{2}T_2)^2 + E_0^2} \\ C_{02} &= \frac{4E_0E_2 - 12T_2(E_0 + E_2)}{\sqrt{(6\sqrt{2}T_2)^2 + E_0^2} \sqrt{(6\sqrt{2}T_2)^2 + E_2^2}} \\ C_{22} &= 1 - \frac{4E_2(6T_2 - E_2)}{(6\sqrt{2}T_2)^2 + E_2^2}. \end{aligned} \quad (56)$$

Moving to the primed basis, we find:

$$\begin{aligned} (b_2^\dagger + b_2)^2 &\rightarrow C_{00} |0'\rangle\langle 0'| + \left(3|\langle 1'|\tilde{1}\rangle|^2 + C_{22}|\langle 1'|\tilde{2}\rangle|^2 \right) |1'\rangle\langle 1'| \\ &\quad + \left(3\langle 1'|\tilde{1}\rangle\langle \tilde{1}|2'\rangle + C_{22}\langle 1'|\tilde{2}\rangle\langle \tilde{2}|2'\rangle \right) |1'\rangle\langle 2'| + \left(3\langle 2'|\tilde{1}\rangle\langle \tilde{1}|1'\rangle + C_{22}\langle 2'|\tilde{2}\rangle\langle \tilde{2}|1'\rangle \right) |2'\rangle\langle 1'| \\ &\quad + \left(3|\langle 2'|\tilde{1}\rangle|^2 + C_{22}|\langle 2'|\tilde{2}\rangle|^2 \right) |2'\rangle\langle 2'|. \end{aligned}$$

Again, we will ignore the energy non-conserving terms proportional to an off-diagonal overlap. We will, though, keep the terms proportional to a non-diagonal overlap in the energy conserving terms for accuracy of the final Hamiltonian. Evaluating the matrix elements gives:

$$\begin{aligned} (b_2^\dagger + b_2)^2 &\xrightarrow{R} C_{00} |0'\rangle\langle 0'| + \frac{3\Delta^2 + C_{22}(-\frac{\delta}{2} + \gamma)^2}{\Delta^2 + (-\frac{\delta}{2} + \gamma)^2} |1'\rangle\langle 1'| \\ &\quad + \frac{3\Delta^2 + C_{22}(\frac{\delta}{2} + \gamma)^2}{\Delta^2 + (\frac{\delta}{2} + \gamma)^2} |2'\rangle\langle 2'|. \end{aligned} \quad (57)$$

We are now ready to look at the full transformed Hamiltonian.

Full Hamiltonian

We can now write down the full Hamiltonian for the system when coupled to an external field mixing the first and second excited state in the rotating frame of the Hamiltonian $H_{\text{ext}} = -\frac{3\omega_{\text{ext}}}{2} |\tilde{0}\rangle\langle\tilde{0}| - \frac{\omega_{\text{ext}}}{2} |\tilde{1}\rangle\langle\tilde{1}| + \frac{\omega_{\text{ext}}}{2} |\tilde{2}\rangle\langle\tilde{2}|$. We start from the Hamiltonian in equation (9) and now insert how the factors containing the bosonic step operators transform under such a transformation, as calculated in the previous section. To sum, up, we found:

$$\begin{aligned} T_1 b_2^\dagger b_2 - T_2 (b_2^\dagger + b_2)^4 + iT_{\text{ext}} \cos(\omega_{\text{ext}}t) (b_2^\dagger - b_2) &\mapsto (E'_1 - E'_0) |1'\rangle\langle 1'| + (E'_2 - E'_0) |2'\rangle\langle 2'| \\ \sqrt{\frac{4\alpha_j}{C_j}} \left(b_j^\dagger b_j + \frac{1}{2} \right) - \frac{\beta_j}{4\alpha_j C_j} (b_j^\dagger + b_j)^4 &\mapsto \frac{1}{2} \left(\sqrt{\frac{4\alpha_j}{C_j}} - \frac{3\beta_j}{\alpha_j C_j} - \omega_{\text{ext}} \right) \sigma_j^z \\ (b_2^\dagger + b_2)(b_j^\dagger + b_j) &\mapsto \frac{k_0 \Delta}{\sqrt{\Delta^2 + (\frac{\delta}{2} - \gamma)^2}} (\sigma_j^+ |0'\rangle\langle 1'| + \sigma_j^- |1'\rangle\langle 0'|) \\ &\quad + \frac{k_2 (\frac{\delta}{2} + \gamma)}{2\gamma} (\sigma_j^+ |1'\rangle\langle 2'| + \sigma_j^- |2'\rangle\langle 1'|) \\ (b_2^\dagger + b_2)^2 (b_j^\dagger + b_j)^2 &\mapsto (C_{00} \mathbb{I}_2 + D_1 |1'\rangle\langle 1'| + D_2 |2'\rangle\langle 2'|) (2 + \sigma_j^z), \end{aligned} \quad (58)$$

where

$$\begin{aligned} D_1 &= \frac{3\Delta^2 + C_{22} \left(-\frac{\delta}{2} + \gamma\right)^2}{\Delta^2 + \left(-\frac{\delta}{2} + \gamma\right)^2} - C_{00} \\ D_2 &= \frac{3\Delta^2 + C_{22} \left(\frac{\delta}{2} + \gamma\right)^2}{\Delta^2 + \left(\frac{\delta}{2} + \gamma\right)^2} - C_{00}. \end{aligned} \quad (59)$$

We remind the reader that we have defined the excited state as $|\uparrow\rangle$ and the ground state as $|\downarrow\rangle$, which explains the sign in front of the σ^z s. We can now write out the full Hamiltonian in the rotating frame, changing the indices from 1, 2, 3 to L, M, R for the sake of visualizing the system as a chain of two qubits with a qutrit in the middle:

$$\begin{aligned} H_{\text{full}} &= \frac{\Delta_L}{2} \sigma_L^z + \Delta_M |1'\rangle\langle 1'| + (\Delta_M + \delta_M) |2'\rangle\langle 2'| + \frac{\Delta_R}{2} \sigma_R^z \\ &\quad + J_{LM_{01}} (\sigma_L^- |1'\rangle\langle 0'| + \sigma_L^+ |0'\rangle\langle 1'|) + J_{RM_{01}} (\sigma_R^- |1'\rangle\langle 0'| + \sigma_R^+ |0'\rangle\langle 1'|) \\ &\quad + J_{LM_{12}} (\sigma_L^- |2'\rangle\langle 1'| + \sigma_L^+ |1'\rangle\langle 2'|) + J_{RM_{12}} (\sigma_R^- |2'\rangle\langle 1'| + \sigma_R^+ |1'\rangle\langle 2'|) \\ &\quad + J_{LM}^{(z)} \sigma_L^z (D_1 |1'\rangle\langle 1'| + D_2 |2'\rangle\langle 2'|) + J_{RM}^{(z)} \sigma_R^z (D_1 |1'\rangle\langle 1'| + D_2 |2'\rangle\langle 2'|), \end{aligned} \quad (60)$$

Here, the diagonal constants are

$$\begin{aligned} \Delta_L &= -\frac{3\beta_1}{\alpha_1 C_1} + \sqrt{\frac{4\alpha_1}{C_1}} - \frac{C_{00}}{64} \frac{E_{J1} \cos\left(\frac{\Phi_{\Sigma 1}}{2}\right)}{\sqrt{\alpha_1 \alpha_2 C_1 (C_1 + C_2 + C_{\text{ext}})}} - \omega_{\text{ext}} \\ \Delta_M &= E'_1 - E'_0 - \frac{D_1}{64} \frac{E_{J1} \cos\left(\frac{\Phi_{\Sigma 1}}{2}\right)}{\sqrt{\alpha_1 \alpha_2 C_1 (C_1 + C_2 + C_{\text{ext}})}} - \frac{D_1}{64} \frac{E_{J2} \cos\left(\frac{\Phi_{\Sigma 2}}{2}\right)}{\sqrt{\alpha_3 \alpha_2 C_2 (C_1 + C_2 + C_{\text{ext}})}} \\ \delta_M &= 2\gamma - \frac{D_2 - D_1}{64} \frac{E_{J1} \cos\left(\frac{\Phi_{\Sigma 1}}{2}\right)}{\sqrt{\alpha_1 \alpha_2 C_1 (C_1 + C_2 + C_{\text{ext}})}} - \frac{D_2 - D_1}{64} \frac{E_{J2} \cos\left(\frac{\Phi_{\Sigma 2}}{2}\right)}{\sqrt{\alpha_3 \alpha_2 C_2 (C_1 + C_2 + C_{\text{ext}})}} \\ \Delta_R &= -\frac{3\beta_3}{\alpha_3 C_2} + \sqrt{\frac{4\alpha_3}{C_2}} - \frac{C_{00}}{64} \frac{E_{J2} \cos\left(\frac{\Phi_{\Sigma 2}}{2}\right)}{\sqrt{\alpha_3 \alpha_2 C_2 (C_1 + C_2 + C_{\text{ext}})}} - \omega_{\text{ext}}, \end{aligned} \quad (61)$$

while the D_i constants are defined in (59) and the rest are

$$\begin{aligned} J_{LM_{01}} &= \left(\frac{1}{8L_1} - \frac{1}{8\tilde{L}_1}\right) \frac{k_0}{2(\alpha_1 \alpha_2 C_1 (C_1 + C_2 + C_{\text{ext}}))^{\frac{1}{4}}} \frac{\Delta}{\sqrt{\Delta^2 + \left(-\frac{\delta}{2} + \gamma\right)^2}} \\ J_{RM_{01}} &= \left(\frac{1}{8L_2} - \frac{1}{8\tilde{L}_2}\right) \frac{k_0}{2(\alpha_3 \alpha_2 C_2 (C_1 + C_2 + C_{\text{ext}}))^{\frac{1}{4}}} \frac{\Delta}{\sqrt{\Delta^2 + \left(-\frac{\delta}{2} + \gamma\right)^2}} \\ J_{LM_{12}} &= \left(\frac{1}{8L_1} - \frac{1}{8\tilde{L}_1}\right) \frac{k_2}{4(\alpha_1 \alpha_2 C_1 (C_1 + C_2 + C_{\text{ext}}))^{\frac{1}{4}}} \frac{\frac{\delta}{2} + \gamma}{\gamma} \\ J_{RM_{12}} &= \left(\frac{1}{8L_2} - \frac{1}{8\tilde{L}_2}\right) \frac{k_2}{4(\alpha_3 \alpha_2 C_2 (C_1 + C_2 + C_{\text{ext}}))^{\frac{1}{4}}} \frac{\frac{\delta}{2} + \gamma}{\gamma} \\ J_{LM}^{(z)} &= -\frac{E_{J1}}{128} \frac{\cos\left(\frac{\Phi_{\Sigma 1}}{2}\right)}{\sqrt{\alpha_1 \alpha_2 C_1 (C_1 + C_2 + C_{\text{ext}})}} \\ J_{RM}^{(z)} &= -\frac{E_{J2}}{128} \frac{\cos\left(\frac{\Phi_{\Sigma 2}}{2}\right)}{\sqrt{\alpha_3 \alpha_2 C_2 (C_1 + C_2 + C_{\text{ext}})}}. \end{aligned} \quad (62)$$

To sum up, we have now, starting from the circuit in Supplementary Fig. 1, calculated the resulting Hamiltonian and added a dynamical tuning of the qutrit via driving of the first and second excited bare qutrit energy levels. In doing so, we first transformed to the rotating picture with respect to the driving field and then to the new mixed qutrit eigenstates, finally obtaining the Hamiltonian above.

Supplementary Note 2: Circuit parameters used in the simulations

In Table 0.1, we have included a list of realistic circuit parameters and the corresponding spin-model parameters they yield. We can split this into three parts, a circuit with Hamiltonian parameters suited to implementing the dissociation

procedure, a circuit implementing the ACSWAP gate, and a circuit with all levels off-resonant, suitable to implementing the STIRAP procedure and CCZ and holonomic gates. Note that for the dissociation and ACSWAP procedures, we are working in the frame rotating with the AC Stark drive frequency, ω_{ext} , and thus the energy terms are reduced accordingly. This of course does not change the (non-trivial) dynamics, since only the relative energy differences are important.

	Circuit parameters	Spin-model parameters
Dissociation, first part (STIRAP)	$L_{1,2} = 19.999 \text{ nH}$, $\tilde{L}_{1,2} = 18.713 \text{ nH}$, $E_{J1,2}/(2\pi) = 185.91 \text{ GHz}$, $E_{Jq1,3}/(2\pi) = 79.515 \text{ GHz}$, $E_{Jq2}/(2\pi) = 27.441 \text{ GHz}$, $C_{1,2} = 55.816 \text{ fF}$, $\Phi_{\Sigma1,2} = -0.43452 \Phi_0$, $C_{\text{ext}} = 2.3411 \text{ fF}$, Dynamical driving off	$\Delta_L/(2\pi) = 15.271 \text{ GHz}$, $\Delta_M/(2\pi) = 13.841 \text{ GHz}$, $\delta_M/(2\pi) = 13.671 \text{ GHz}$, $\Delta_R/(2\pi) = 15.271 \text{ GHz}$, $J_{\alpha M_{01}}/(2\pi) = 9.2737 \text{ MHz}$, $J_{\alpha M_{12}}/(2\pi) = 12.996 \text{ MHz}$, $J_{\alpha M}^{(z)}/(2\pi) = -20.433 \text{ MHz}$, $D_1 = 1.9877$, $D_2 = 3.9754$, $\max(\Omega_{1,2})/(2\pi) = 20 \text{ MHz}$
Dissociation, second part (two-photon resonance)	$L_{1,2} = 20.000 \text{ nH}$, $\tilde{L}_{1,2} = 16.949 \text{ nH}$, $E_{J1,2}/(2\pi) = 32.371 \text{ GHz}$, $E_{Jq1,3}/(2\pi) = 109.74 \text{ GHz}$, $E_{Jq2}/(2\pi) = 108.94 \text{ GHz}$, $C_{1,2} = 55.935 \text{ fF}$, $\Phi_{\Sigma1,2} = 0.27790 \Phi_0$, $C_{\text{ext}} = 71.773 \text{ fF}$, $A_{\text{ext}}/(4\alpha_2(C_1 + C_2 + C_{\text{ext}}))^{-1/4} = 0.1000$, $\omega_{\text{ext}}/(2\pi) = 14.674 \text{ GHz}$	In the frame rotating with ω_{ext} : $\Delta_L/(2\pi) = 0.46529 \text{ GHz}$, $\Delta_M/(2\pi) = 0.088376 \text{ GHz}$, $\delta_M/(2\pi) = 0.84222 \text{ GHz}$, $\Delta_R/(2\pi) = 0.46529 \text{ GHz}$, $J_{\alpha M_{01}}/(2\pi) = 15.0203 \text{ MHz}$, $J_{\alpha M_{12}}/(2\pi) = 17.114 \text{ MHz}$, $J_{\alpha M}^{(z)}/(2\pi) = -6.4890 \text{ MHz}$, $D_1 = 2.6636$, $D_2 = 3.3015$
CCNOT/CCZ	Same as during STIRAP.	Same as for STIRAP, except $\Omega_1/(2\pi) = 6 \text{ MHz}$
ACSWAP (first part of CCSWAP)	$L_{1,2} = 16.049 \text{ nH}$, $\tilde{L}_{1,2} = 18.988 \text{ nH}$, $E_{J1,2}/(2\pi) = 56.08 \text{ GHz}$, $E_{Jq1,3}/(2\pi) = 155.22 \text{ GHz}$, $E_{Jq2}/(2\pi) = 135.33 \text{ GHz}$, $C_{1,2} = 56.619 \text{ fF}$, $\Phi_{\Sigma1,2} = 0.49999 \Phi_0$, $C_{\text{ext}} = 90.011 \text{ fF}$, $A_{\text{ext}}/(4\alpha_2(C_1 + C_2 + C_{\text{ext}}))^{-1/4} = 0.10000$, $\omega_{\text{ext}}/(2\pi) = 14.367 \text{ GHz}$	In the frame rotating with ω_{ext} : $\Delta_L/(2\pi) = 0.9113 \text{ GHz}$, $\Delta_M/(2\pi) = -0.0798 \text{ GHz}$, $\delta_M/(2\pi) = 0.9121 \text{ GHz}$, $\Delta_R/(2\pi) = 0.9113 \text{ GHz}$, $J_{\alpha M_{01}}/(2\pi) = 14.311 \text{ MHz}$, $J_{\alpha M_{12}}/(2\pi) = 15.173 \text{ MHz}$, $J_{\alpha M}^{(z)}/(2\pi) = -0.601 \text{ kHz}$, $D_1 = 2.8377$, $D_2 = 3.12544$
Holonomic gate (double-controlled)	Same as during STIRAP	Same as for STIRAP, except $\Omega_{1,2}/(2\pi) = 15 \text{ MHz}$

Table 0.1: A table of realistic parameters and the corresponding Hamiltonian parameters used in each implementation. In all simulations, we have included finite relaxation and coherence times set to $T_1 = 31 \mu\text{s}$ and $T_2 = 35 \mu\text{s}$, respectively. The parameters of the second part of the CSWAP is not shown, but is obtained by varying only the external parameters relative to the first part. The resulting parameters are similar to what is shown for the CCNOT gate implementation.

Supplementary Note 3: Direct Dissociation to Entanglement

We wish to obtain an entangled state between the state where qubit one and three is in the excited state and the state where they are both in the ground state. Since the Hamiltonian conserves the total projection of spin, we start in the state $|\downarrow 2 \downarrow\rangle$. We look at the matrix representation of our Hamiltonian in the basis $\{|\downarrow 2 \downarrow\rangle, |\downarrow 1 \uparrow\rangle, |\uparrow 1 \downarrow\rangle, |\uparrow 0 \uparrow\rangle\}$. If we assume the system to be symmetric, i.e. we do not distinguish between $\alpha = L$ and $\alpha = R$, and further assume the states to be resonant, i.e. $\Delta_M = \Delta_R = \Delta_L = \delta_M$, the contribution from these energy terms is proportional to the identity and we are left with the matrix representation of the XX and ZZ-terms, which we can easily diagonalize to find the eigenvalues. In the simplified case $J_{\alpha M_{01}} = J_{\alpha M_{12}} = J_{\alpha M}$ and $D_1 = D_2 = 1$ (This is not essential, and is only chosen as to ease the readability of the analysis. The equation for $D_2 J_{\alpha M}^{(z)}$ in the main text is the result in the non-simplified case), the eigenvalues are:

$$E_1 = 0 \quad , \quad E_2 = -2J_{\alpha M}^{(z)} \quad , \quad E_3 = -J_{\alpha M}^{(z)} - \lambda \quad \text{and} \quad E_4 = -J_{\alpha M}^{(z)} + \lambda, \quad (63)$$

where

$$\lambda = \sqrt{4J_{\alpha M}^2 + J_{\alpha M}^{(z)2}}. \quad (64)$$

The associated eigenvectors are

$$\begin{aligned} |v_1\rangle &= \frac{1}{\sqrt{2}} \begin{pmatrix} 0 \\ 0 \\ -1 \\ 1 \end{pmatrix}, \quad |v_2\rangle = \frac{1}{\sqrt{2}} \begin{pmatrix} -1 \\ 1 \\ 0 \\ 0 \end{pmatrix}, \quad |v_3\rangle = \sqrt{\frac{\lambda - J_{\alpha M}^{(z)}}{4\lambda}} \begin{pmatrix} \frac{2J_{\alpha M}}{J_{\alpha M}^{(z)} - \lambda} \\ \frac{2J_{\alpha M}}{J_{\alpha M}^{(z)} - \lambda} \\ 1 \\ 1 \end{pmatrix} \\ \text{and } |v_4\rangle &= \sqrt{\frac{\lambda + J_{\alpha M}^{(z)}}{4\lambda}} \begin{pmatrix} \frac{2J_{\alpha M}}{J_{\alpha M}^{(z)} + \lambda} \\ \frac{2J_{\alpha M}}{J_{\alpha M}^{(z)} + \lambda} \\ 1 \\ 1 \end{pmatrix}. \end{aligned} \quad (65)$$

We can now find

$$\begin{aligned} \langle f | e^{-iHt} | \downarrow 2 \downarrow \rangle &= \sum_{n,m=1}^4 \langle f | v_n \rangle \langle v_n | e^{-iHt} | v_m \rangle \langle v_m | \downarrow 2 \downarrow \rangle \\ &= \sum_{n=1}^4 \langle f | v_n \rangle e^{-iE_n t} \langle v_n | \downarrow 2 \downarrow \rangle, \end{aligned} \quad (66)$$

where $|f\rangle$ is one of the four basis states mentioned earlier. From this, the complete time development of $|\downarrow 2 \downarrow\rangle$ is recovered analytically. Specifically, we have

$$|\langle \downarrow 2 \downarrow | e^{-iHt} | \downarrow 2 \downarrow \rangle|^2 = \frac{1}{4} \left(\cos(J_{\alpha M}^{(z)} t) + \cos(\lambda t) \right)^2 + \frac{1}{4} \left(\sin(J_{\alpha M}^{(z)} t) + \frac{J_{\alpha M}^{(z)}}{\lambda} \sin(\lambda t) \right)^2$$

and

$$|\langle \uparrow 0 \uparrow | e^{-iHt} | \downarrow 2 \downarrow \rangle|^2 = \frac{1}{4} \left(\cos(J_{\alpha M}^{(z)} t) - \cos(\lambda t) \right)^2 + \frac{1}{4} \left(\sin(J_{\alpha M}^{(z)} t) - \frac{J_{\alpha M}^{(z)}}{\lambda} \sin(\lambda t) \right)^2.$$

Because $\lambda = \sqrt{4J_{\alpha M}^2 + J_{\alpha M}^{(z)2}}$ we, for a general $J_{\alpha M}^{(z)}$, expect the probabilities to have a chaotic behavior. We ask ourselves if there exists a certain value of $J_{\alpha M}^{(z)} > 0$ where we can find a time t at which

$$|\langle \downarrow 2 \downarrow | e^{-iHt} | \downarrow 2 \downarrow \rangle|^2 = |\langle \uparrow 0 \uparrow | e^{-iHt} | \downarrow 2 \downarrow \rangle|^2 = \frac{1}{2} \quad (67)$$

and

$$\frac{d}{dt} |\langle \downarrow 2 \downarrow | e^{-iHt} | \downarrow 2 \downarrow \rangle|^2 = \frac{d}{dt} |\langle \uparrow 0 \uparrow | e^{-iHt} | \downarrow 2 \downarrow \rangle|^2 = 0. \quad (68)$$

From the first equality in (67), we find the condition

$$\cos(\lambda t) \cos(J_{\alpha M}^{(z)} t) = -\frac{J_{\alpha M}^{(z)}}{\lambda} \sin(\lambda t) \sin(J_{\alpha M}^{(z)} t), \quad (69)$$

while we from equation (68) get

$$\begin{aligned} \sin(\lambda t) \left(\cos(J_{\alpha M}^{(z)} t) + \cos(\lambda t) \right) &= 0 = \sin(\lambda t) \left(\cos(J_{\alpha M}^{(z)} t) - \cos(\lambda t) \right) \\ \Rightarrow \sin(\lambda t) &= 0 \quad \text{or} \quad \cos(J_{\alpha M}^{(z)} t) = \cos(\lambda t) = 0. \end{aligned} \quad (70)$$

Here, the second option implies that $\sin(J_{\alpha M}^{(z)} t) = \pm \sin(\lambda t) = \pm 1 \neq 0$, which is not compatible with the condition (69).

Therefore, we must have $\sin(\lambda t) = 0$ and from (69) also $\cos(J_{\alpha M}^{(z)} t) = 0$. This means that we have two conditions on our time $t > 0$:

$$t = n \frac{\pi}{\lambda} \quad \text{and} \quad t = m \frac{\pi}{2J_{\alpha M}^{(z)}}, \quad n \in \mathbb{N}, \quad m = 1, 3, 5, \dots \quad (71)$$

We solve this for $J_{\alpha M}^{(z)}$:

$$\begin{aligned} n \frac{\pi}{\lambda} &= m \frac{\pi}{2J_{\alpha M}^{(z)}} \Rightarrow 4n^2 J_{\alpha M}^{(z)2} = (4J_{\alpha M}^2 + J_{\alpha M}^{(z)2})m^2 \\ \Rightarrow J_{\alpha M}^{(z)} &= \frac{2J_{\alpha M}}{\sqrt{4n^2/m^2 - 1}}, \end{aligned} \quad (72)$$

where $n = 1, 2, 3, \dots$ and $m = 1, 3, 5, \dots$ with the further condition to keep the time real $4n^2/m^2 > 1 \Rightarrow n > m/2$. This is plotted for $n = m = 1$ in Supplementary Fig. 2 for arbitrary values of parameters for proof of concept.

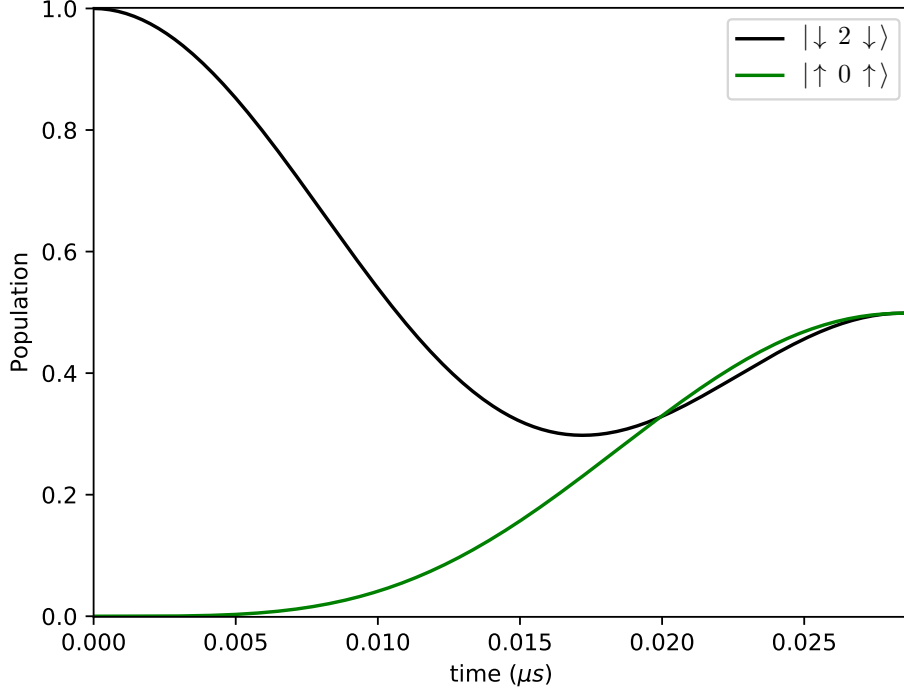
Supplementary Note 4: Analysis of the CSWAP

Assuming that the excited states of the outer qubits are in resonance with the second excited state of the qutrit ($\Delta_L \simeq \delta_M \simeq \Delta_R$) while the qutrit ground state is far detuned from the rest, we can move to the interaction picture of the diagonal in equation (60), ignoring these terms and also all terms involving the ground state ($|0\rangle$) of the qutrit. We also choose to assume symmetry between both ends of the chain, so e.g. $J_{LM_{12}} = J_{RM_{12}} = J_{\alpha M_{12}}$, and that $J_{\alpha M}^{(z)} = 0$. A non-zero ZZ-coupling will make the states with the qubits in the same state slightly detuned, introducing a non-perfect transition. This can be remedied a bit by choosing $\Delta_\alpha = \delta_M - 2\frac{D_1+D_2}{2}J_{\alpha M}^{(z)}$, but because in general $D_1 \neq D_2$, this detuning can not be fixed completely. In the basis $\{|\downarrow 1 \downarrow\rangle, |\uparrow 1 \downarrow\rangle, |\downarrow 2 \downarrow\rangle, |\downarrow 1 \uparrow\rangle, |\uparrow 2 \downarrow\rangle, |\uparrow 1 \uparrow\rangle, |\downarrow 2 \uparrow\rangle, |\uparrow 2 \uparrow\rangle\}$, the interaction part of the Hamiltonian can be written very simply:

$$H_I = \begin{pmatrix} 0 & 0 & 0 & 0 & 0 & 0 & 0 & 0 \\ 0 & 0 & J_{\alpha M_{12}} & 0 & 0 & 0 & 0 & 0 \\ 0 & J_{\alpha M_{12}} & 0 & J_{\alpha M_{12}} & 0 & 0 & 0 & 0 \\ 0 & 0 & J_{\alpha M_{12}} & 0 & 0 & 0 & 0 & 0 \\ 0 & 0 & 0 & 0 & 0 & J_{\alpha M_{12}} & 0 & 0 \\ 0 & 0 & 0 & 0 & J_{\alpha M_{12}} & 0 & J_{\alpha M_{12}} & 0 \\ 0 & 0 & 0 & 0 & 0 & J_{\alpha M_{12}} & 0 & 0 \\ 0 & 0 & 0 & 0 & 0 & 0 & 0 & 0 \end{pmatrix}. \quad (73)$$

Notice the block matrix form where the two 3×3 matrices represent irreducible subspaces. Furthermore, they are equal in form, so when performing the time evolution $e^{-iH_I t}$ we only have to exponentiate one of these irreducible sub-matrices. It is easily found that:

$$\exp \left[-i \begin{pmatrix} 0 & J_{\alpha M_{12}} & 0 \\ J_{\alpha M_{12}} & 0 & J_{\alpha M_{12}} \\ 0 & J_{\alpha M_{12}} & 0 \end{pmatrix} t \right] = \frac{1}{2} \begin{pmatrix} \cos(\sqrt{2}J_{\alpha M_{12}}t) + 1 & -i\sqrt{2}\sin(\sqrt{2}J_{\alpha M_{12}}t) & \cos(\sqrt{2}J_{\alpha M_{12}}t) - 1 \\ -i\sqrt{2}\sin(\sqrt{2}J_{\alpha M_{12}}t) & 2\cos(\sqrt{2}J_{\alpha M_{12}}t) & -i\sqrt{2}\sin(\sqrt{2}J_{\alpha M_{12}}t) \\ \cos(\sqrt{2}J_{\alpha M_{12}}t) - 1 & -i\sqrt{2}\sin(\sqrt{2}J_{\alpha M_{12}}t) & \cos(\sqrt{2}J_{\alpha M_{12}}t) + 1 \end{pmatrix}. \quad (74)$$



Supplementary Figure 2: Probability of occupation in the case $J_{\alpha M}^{(z)} = 2J_{\alpha M}/\sqrt{3}$. We notice that the desired entangled state is reached at $t = \pi/\lambda = \pi/2J_{\alpha M}^{(z)} \approx 1.36 \frac{1}{J_{\alpha M}} \approx 0.028 \mu\text{s}$.

Letting the qutrit start in the ground state, we can now find

$$e^{-iH_I t} |\downarrow 1 \downarrow\rangle = |\downarrow 1 \downarrow\rangle \quad (75)$$

$$e^{-iH_I t} |\uparrow 1 \downarrow\rangle = \cos^2\left(\frac{J_{\alpha M_{12}}}{\sqrt{2}}t\right) |\uparrow 1 \downarrow\rangle - \frac{i}{\sqrt{2}} \sin\left(\sqrt{2}J_{\alpha M_{12}}t\right) |\downarrow 2 \downarrow\rangle - \sin^2\left(\frac{J_{\alpha M_{12}}}{\sqrt{2}}t\right) |\downarrow 1 \uparrow\rangle \quad (76)$$

$$e^{-iH_I t} |\uparrow 1 \uparrow\rangle = -\frac{i}{\sqrt{2}} \sin\left(\sqrt{2}J_{\alpha M_{12}}t\right) (|\uparrow 2 \downarrow\rangle + |\downarrow 2 \uparrow\rangle) + \cos\left(\sqrt{2}J_{\alpha M_{12}}t\right) |\uparrow 1 \uparrow\rangle. \quad (77)$$

We wish to obtain a -CSWAP, so we require $|\langle \downarrow 1 \uparrow | e^{-iH_I T} | \uparrow 1 \downarrow \rangle|^2 = 1$, thus we must choose the operation time to be $T = \frac{\pi}{\sqrt{2}J_{\alpha M_{12}}}$. Inserting this into the equations above, we get

$$\langle \downarrow 1 \uparrow | e^{-iH_I T} | \uparrow 1 \downarrow \rangle = \langle \uparrow 1 \uparrow | e^{-iH_I T} | \uparrow 1 \uparrow \rangle = -1 = -\langle \downarrow 1 \downarrow | e^{-iH_I T} | \downarrow 1 \downarrow \rangle. \quad (78)$$

This last matrix element has the wrong sign, so if we tried to perform a -CSWAP between the outer qubits in different superpositions of the ‘up’ and ‘down’ state, we would obtain an unfortunate relative sign change. This can be seen by assuming the left qubit starts in the superposition

$$|\psi_L\rangle = a|\uparrow\rangle + b|\downarrow\rangle, \quad (79)$$

while the right qubit starts in the superposition

$$|\psi_R\rangle = c|\uparrow\rangle + d|\downarrow\rangle. \quad (80)$$

Here, a, b, c and d are complex coefficients. The total starting state of the system is then the factorizable state

$$(a|\uparrow\rangle + b|\downarrow\rangle) |1\rangle (c|\uparrow\rangle + d|\downarrow\rangle) = ac|\uparrow 1 \uparrow\rangle + ad|\uparrow 1 \downarrow\rangle + bc|\downarrow 1 \uparrow\rangle + bd|\downarrow 1 \downarrow\rangle. \quad (81)$$

Operating on this state with the unitary operator $e^{-iH_I T}$ now gives:

$$-ac|\uparrow 1 \uparrow\rangle - ad|\downarrow 1 \uparrow\rangle - bc|\uparrow 1 \downarrow\rangle + bd|\downarrow 1 \downarrow\rangle. \quad (82)$$

This state is not factorizable because of the sign difference between the first term and the rest, and therefore does not have a simple interpretation as the system where a SWAP operation has been performed.

This can be fixed by first operating with a CCZ gate on the system so that only this specific state ($|\downarrow 1 \downarrow\rangle$) obtains a sign change. This of course requires that the states are first moved out of resonance, but this is already required in order to catch the system in the swapped state. We then obtain the state

$$-ac|\uparrow 1 \uparrow\rangle - ad|\downarrow 1 \uparrow\rangle - bc|\uparrow 1 \downarrow\rangle - bd|\downarrow 1 \downarrow\rangle = -(c|\uparrow\rangle + d|\downarrow\rangle)|1\rangle(a|\uparrow\rangle + b|\downarrow\rangle). \quad (83)$$

It is clear that the states of the outer qubits have been swapped, just as we wanted!

We thus end up with a CSWAP gate in the interaction picture of H_0 with a two-step operation scheme and with the control “bit” being comprised of the states $|0\rangle$ and $|1\rangle$ of the qutrit (or, equivalently, the states $|1\rangle$ and $|2\rangle$ if we instead apply the CCZ so only the state $|\uparrow 1 \uparrow\rangle$ receives a sign change). By symmetry, the topmost excited qutrit state $|2\rangle$ will also allow transfer, but here the state $|\uparrow 2 \uparrow\rangle$ will need a sign change.

A simulation of the CSWAP/Fredkin gate is shown in the main text, where we get a fidelity of around 0.95 for a perfect SWAP operation when the qutrit starts in the first excited state, as predicted by the analytical investigation above.